RECEIVER GAIN STABILITY

MARCH 2001

SUMMARY

Summary of Receiver Gain Stability

Telescope	Receiver	Total Power Stability	Time Scale	Environment
BIMA[1]	SIS mixer @ 100 GHz	4e-4	1-1000 sec	lab
BIMA[1]	SIS mixer @ 100 GHz	1e-3	1-1000 sec	telescope
BIMA[1]	SIS mixer @ 100 GHz	2e-3	1 day	lab
BIMA[1]	SIS mixer	1e-2	1-1000 sec	n/a
NRAO[2]	SIS mixer @ 97 GHz (3mm-high/ch-1)	4e-4	1 sec	lab
NRAO[2]	SIS mixer @ 89 GHz (3mm-low/spare)	3e-3	1 sec	lab
NRAO[2]	SIS mixer @ 75 GHz (3mm-low/ch-2)	7e-4	1 sec	lab
AST/RO[3]	SIS mixer @ 810 GHz	9e-4	1000 sec	lab

Temperature Stability of Components[4]

Component	A gain fluctuation of 1e-4 is produce by a temperature change of:
SIS mixer operating at 3.8 K	0.002 K
1.8 GHz HEMT amplifier at 14 K	0.012 K
Amplifier chain and detector at 300 K	0.008 K

(1) R. Plambeck, Personal comm. and refer. (4)
(2) 12-meter telescope staff
(3) C. Walker, Steward Observatory
(4) Interferometer Phase Correction From Receiver Total Power Measurements, R. Plambeck et al., 1996 URSI abstract
Gain and Phase Stabilities of Components Used in the BIMA array, B. Frye et al., MMA memo #131

BIMA

INTERFEROMETER PHASE CORRECTION FROM RECEIVER TOTAL POWER MEASUREMENTS

R. Plambeck* R. Forster B. Frye J. Lugten W. Welch
M. Wright
Radio Astronomy Lab
University of California
Berkeley, CA 94720

Abstract Submission Form

1996 National Radio Science Meeting

Reference # 0000
Session 0.00

The Berkeley-Illinois-Maryland Array allows observations at millimeter wavelengths with antenna separations of up to 1.2 km. At such long baselines the array sensitivity is limited by atmospheric phase fluctuations – due largely to tropospheric water vapor – with time scales of a few seconds to tens of minutes. The same molecules of water vapor which cause the phase delays also emit radiation; hence it is possible to monitor variations in the atmospheric path length by measuring changes in the sky brightness at each antenna. This is done most simply by monitoring the receiver total powers at the observing frequency.

The conversion factor from sky brightness to phase delay depends on the observing frequency and the altitude distribution of water vapor. At 100 GHz, a 1 K increase in sky brightness typically corresponds to 200° of phase delay. Thus, in order to determine the atmospheric phase delay with an accuracy of 10°, one must measure the sky brightness with an accuracy of 0.05 K. This is only 3×10^{-4} of the typical DSB system temperature of 150 K, requiring that the receiver gains be stable to this level. Very good temperature stabilization of all components is required to achieve such gain stability. Tests of the BIMA receivers show that a fractional gain fluctuation of 10^{-4} is produced by the following temperature changes:

SIS mixer operating at 3.8 K	0.002 K
1.8 GHz HEMT amplifier at 14 K	0.012 K
amplifier chain and detector at 300 K	0.008 K

In lab tests we have succeeded in stabilizing temperatures to these levels, and find that the receiver total power fluctuations are then approximately 4×10^{-4} on time scales of 1–1000 sec, 2×10^{-3} on time scales of a day. If this level of gain stability can be achieved routinely on the telescopes, it should be possible to compensate for many of the atmospheric fluctuations at long baselines.

1. (a)
   R. Plambeck
   Radio Astronomy Lab
   University of California
   Berkeley, CA 94720 USA
   plambeck@fringe.berkeley.edu
   (b) 510-642-3441
   (c) 510-642-3411
2. J
3. (a) Tropospheric phase calibration for interferometers
4. I, Program chair: David Woody
5. No special instructions

Date received: 23 May 95
Date formatted: September 22, 1995
Form version: 1.0

Subject: Re: ALMA Receiver gain stability
Date: Mon, 26 Mar 2001 20:08:36 -0800 (PST)
From: dick plambeck 449 <plambeck@astron.berkeley.edu>
To: aperfett@nrao.edu
CC: wright@mars.berkeley.edu, welch@mars.berkeley.edu

Dear Antonio,

Mel Wright forwarded your query about receiver gain stability to me.

Attached is the abstract of a talk I gave at the 1996 URSI meeting reporting on the receiver gain stability at BIMA. By carefully temperature-stabilizing the SIS mixer, HEMT amplifier, and room temperature components on one of our receivers, we achieved a total power stability of a few parts in 10^4 in the lab over periods of 1000 sec. In real life, with receivers on the telescopes, the stability was probably closer to 1 part in 10^3 over periods of 1000 sec.

ALMA memo 131, by Frye et al., describes in considerable detail the thermal tests which were done on the room temperature components. This memo seems not to have been scanned into the system -- I couldn't retrieve it from the ALMA web page, but presumably it is on file somewhere at NRAO.

Since 1996 we have replaced all our SIS mixers with more sensitive ones. Because the new 3mm mixers begin to saturate even on a 70 K load (see Engargiola and Plambeck 1998, Proc. SPIE, 3357, 508), we bias them on the side of the gain peaks, which makes them exquisitely sensitive to temperature fluctuations. Thus, the total power stability of the current BIMA receivers is probably of order 1 part in 100.

Presuming that ALMA uses mixers with series arrays of several junctions at the longer wavelengths, so that saturation is not a big problem, it seems to us that achieving 1 part in 10^4 stability is possible, but it will require a substantial effort to temperature-regulate not only the cryogenic components, but also those at room temperature.

Best wishes,
Dick Plambeck

July 1995 MMA memo # 131

(1)

Gain and phase stabilities of some components used in the BIMA array. These data may be helpful in system considerations for the MMA.

B. Frye, R. Forster, J. Lugten, L. Mundy, R. Plambeck, D. Thornton, and J. Welch

The following sections summarize various stability measurements on BIMA components and subsystems. The first section describes gain stability measurements of individual components of the IF system and then summarizes the overall IF stability. The second section discusses phase/temperature stability of some components. The third section discusses measurements on optical fiber. The fourth secion describes some overall receiver gain/temperature measurements.

I. First, a summary of the temperature sensitivity of the gains of the IF components on the IF plate between the dewar and the total power dectector. Below is a block diagram of the layout. The temperature/gain sensitivity was measured using an environmental chamber. The test of each component consisted of measuring its gain throughout the cycle: (1) increase of temperature from 25.0 to 35.0 C in 10 minutes (2) steady temperature at 35.0 C for 10 minutes, then (3) decrease temperature from 35.0 to 25.0 C in 10 minutes, (4) steady temperature at 25.0 C for 5 - 10 minutes. Temperature changes occurred at a constant rate. The 10 minutes spent at each temperature seemed to be adequate for the temperature of each device to stabilize.

Gain measurements were made at a fixed frequency, either 600 MHz or 1900 MHz, with an HP 8753A Network analyzer. Power detector output was measured with a Fluke voltmeter. The power detector is installed in the second IF amplifier box.

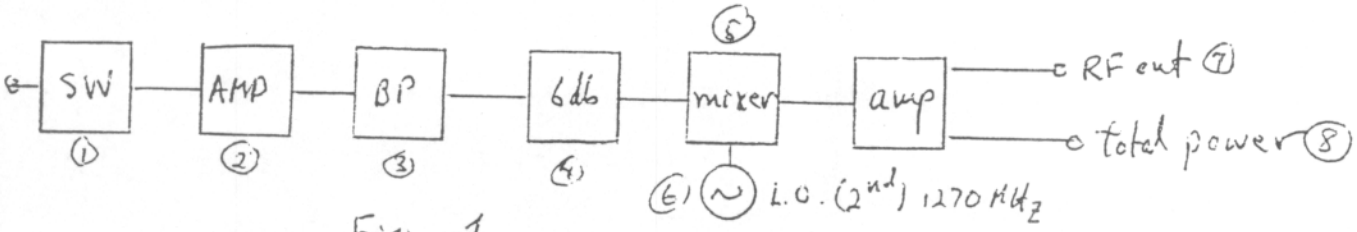

Figure 1

Gain/temperature sensitivities.

1. Minicircuits switch (ZSDR-425): (dG/G)/dT < .0003 db/deg C

2. 1.3 - 2.2 GHz first amplifier. This contains 2 NEC UTC27xx amplifiers: (dG/G)dT = -.0091 db/deg C

3. Bandpass Filter (KWM FSCM 56216): (dG/G)dT = -.005 db/deg

4. 6 db pad: dG/G = 0

5. Anzac MDC-169 mixer: (dG/G)dT = -.0015 db/deg

6. 1270 Oscillator: Output power: (dP/P)dT = -.019 db/deg. The MDC-169 mixer is saturated, reducing this effect by a factor of about ten at the mixer to: -.0014 db/deg

7. Second IF Amp. This contains 3 NEC UTC27xx and one MSA 0420 (Avantec) amplifiers, a 9 pole 70 MHz Hi-pass filter, and a 9-pole 900 MHz low pass filter. The circuit board is low loss ceramic, as it is for the above amplifier. (dG/G)dT = -.010 db/deg

8. Power detector in the final amp: (dDC/DC)dT = -.7%/deg. No DC drift with temperature, only the multiplicative factor changes with temperature.

total gain

The overall drift with temperature is: -.027 db/deg or -.62%/deg.

All of the coefficients are negative, and they simply add. Adding the effect of the power detector, -.7%/deg, gives a total of -1.32%/deg for the overall total power sensitivity.

The IF components are located on a plate within an enclosure which has its temperature regulated. The best regulated front-end IF plate maintains a peak to peak temperature variation of .02K over 24 hours. It's about half that over an hour, .01K. This leaves us with an overall gain stability of -.013% p-p for times of the order of an hour.

Here is a break-down showing the various contributions to the gain/temperature sensitivity of the 1.3 - 2.2 GHz amplifier, item 2 above. Each active unit in the system has its own voltage regulator, in this case a Motorola MC78L05AC, to increase stability. The overall power supply is, of course, also stable. The two amplifiers are from NEC:UTC2711 and UTC2712. Their gain sensitivities are -.002 and -.003 db/degK, respectively. Their power supply sensitivities are both .0015 db/mV. The regulator drifts by -1.0mV/degK, which tanslates to -.003db/degK for the two amplifiers. The ceramic circuit board for this length of trace has a sensitivity of -.001 db/degK at 1.7 GHz. (Note that this is an order of magnitude less than what one gets with normal fiberglass boards). The total is just -.009 db/degK, as measured. This component is typical.

II. Here are measurements of the phase stability of some components with respect to temperature.

1. A 10 MHz distribution amplifier: 0.1 deg phase/degK at each port. This ultimately is multiplied up to be the reference of the second LO at 1270 MHz on each antenna, where the phase is therefore 12.7 deg/degK.

2. A multiple doubler which produces 20, 40, and 80 MHz from the 10 MHz. The 20 and 80 are phase lock offsets. The 20 MHz is 0.75 deg/degK. It is the offset for the 10 GHz intermediate lock loop, and so is multiplied by 25 at 250 GHz, giving a sensitivity of 19 deg/degK. The 40 MHz has a sensitivity of -.25 deg/degK. It is multiplied up to produce the reference for the 1270 MHz LO, giving a sensitivity of -8deg/degK.

3. An Anzac model DS 4-4 four way power splitter at 730 MHz: less than .01deg/degK. (This is a freebe. We don't use it anymore, but we had the measurements.)

The array uses a system of filters to put all the signals onto one coax cable for the connection between the lab and each antenna. These filters have the following phase/temperature sensitivities.

4. The input port to the 1100-1260 MHz high frequency reference port: .16deg/deg at 1180 Mhz, 34 deg/degK at 250 GHz.

5. The input port to the 10 MHz port: .025deg/degK, 3 deg/degK at 1270 MHz.

6. The input port to the 70-900MHz IF port, at 600 MHz: less than .013deg/degK

7. The bandpass filter, item 3 from the first list: 0.1 deg/degK @ 1.75 GHz

8. The second IF amplifier, item 7 from the first list: less than .03deg/degK, at 600 MHz.

9. The L-band amplifier, item 2 from the first list: less than 0.1 deg/deg, at 1.9 GHz.

Items 1,2,4,5,6,7,8, and 9 are located on the front-end IF plate, and so their variations are reduced by a factor of 100 to small values. There are also filter units in the lab, with the properies of 4 and 5, which are not so well

regulated. However, they drift slowly, changing by less than 0.2K in a half hour, and are tolerable.

III. For our more distant stations, we are using optical fiber for the connections of all the signals between the lab and the antenna. The phase reference, at 1100 - 1260 MHz, and the IF, 70 - 900 MHz, use single mode fiber, and the low frequency signals, 10 MHz reference, telemetry at 1 MHz, and TV and communication in a 20-70MHz band, use multimode.

A harmonic of the 10 MHz is the phase reference for the 1270 MHz second LO, and so we tested the phase stability of the multimode fiber. The phase sensitivity of the fiber, referred to 1270 GHz, is 4deg/degK for a 100 foot length of the fiber. This is the length of the run from a pit up to the receiver on one antenna, and it is the length whose temperature changes. The remainder of the cable is burried at a depth of about 18 inches and is relatively stable. The variation of 4 deg/degK will be corrected using delay measurements on the single mode fiber used for the reference. These fibers are packaged together, and so this should work, although we haven't tried it yet.

We also made temperature/phase tests on the single mode fiber. It is the tightly jacketed version, with several fibers in the bundle. We found that the sensitivity is about 10 deg/degK per meter length at 100 GHz. This is worse than coax and requires regulation of some kind. The attached panel of figures, 2a, 2b ,2c ,and 2d, shows measurements of the one way phase on the fiber, in turns at 1.2 GHz. These are for the runs to antennas 6 and 7 which were connected to the fiber. These measurements are made with our line length measuring system. THe short term measurement noise has an RMS of about 1 degree at 100 Ghz. The abcissa is time, 200 measurements, each of which is 1.5 sec in duration. Figures 2a and 2b show the temperature drift effects with the two antennas stationary. Figures 2c, and 2d show the mechanical effect of beginnig a slew at full speed.

Although the tightly jacketed fiber has a poor temperature stability, it is often recommended because it is sturdy. For the underground burial, the gel filled version, which is more stable, is probably a good choice. Vertical runs of this style are not recommended because all the weight may fall on just one fiber. The highly stabilized fiber made by Sumitomo is too rigid for our bicycle chain azimuth cable wrap.

IV. An overall gain stability measurement has been made on one of the receiver front-ends at 100 GHz. It includes everything from a load at the receiver input through to the total power detector on the IF plate. The input load is an absorber whose physical temperature is recorded. Figure 3 shows the total output power as a function of time. The input load is mounted on a thermo-electric cooler/heater, whose temperature can be changed. Near the beginning of the run, there is a 0.5K pulse to calibrate the system. Load temperature is on the right, output total power on the left. The measured load temperature is shown by the dotted line. After the pulse is turned off, the load temperature drifts in time and appears on the total power. The magnitude of a deflection of 1/1000 is shown in the lower lefthand corner.

The temperature regulation of components in the dewar is as follows. The SIS mixer block temperature is 3.6K with an RMS fluctuation of 4mK. We find that the lower the operating temperature, the smaller is the gain fluctuation for a given temperature fluctuation. The HEMT first IF stage is thermally connected to the second refrigerator stage. It's average temperature here is 13.6K, and its RMS fluctuation is 2mK. Active regulation is necessary to achieve this stability, because the temperature of the

Gifford-McMahon refrigerator swings up and down with the motion of the displacer. The local oscillator power is regulated with a Hughes ferrite modulator.

The sample time for the output in Figure 3 is 0.3 seconds, and the bandwidth is 830 MHz, predicting a minimum RMS thermal fluctuation of 6 x 10**-5. The actual RMS fluctuations are about 2 x 10**-4, 3-4 times larger. They also have a strong low frequency component, probably 1/f, although we did not calculate it. These are evidently the residual gain fluctuations.

From these results, one can estimate the atmospheric phase vs total power sensitivity. The theoretical prediction is that at 100 Ghz 1 degK of atmospheric brightness temperature fluctuation will result in about 200 degrees of phase fluctuation. In addition, whereas this experiment was done with a 296K load, the expected atmospheric brightness is more like 45k. (Tau=.12 and secz=1.4, sort of average). With a receiver T(DSB)=70K, the system temperature on the sky will be about one third its value during the experiment. With this correction, the deflection on the right side of Figure 3 is therefore the equivalent of a 13 degree phase change. Evidently, this deflection represents something like the peak phase fluctuation to be expected.

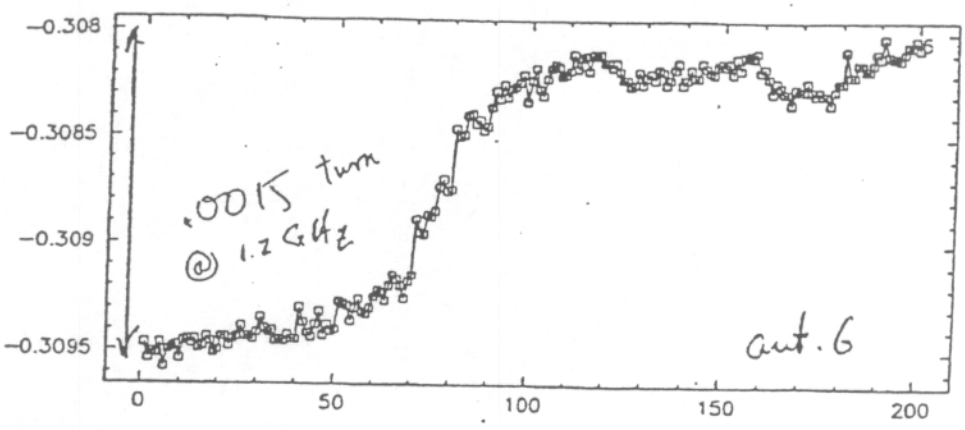

Fig 2a

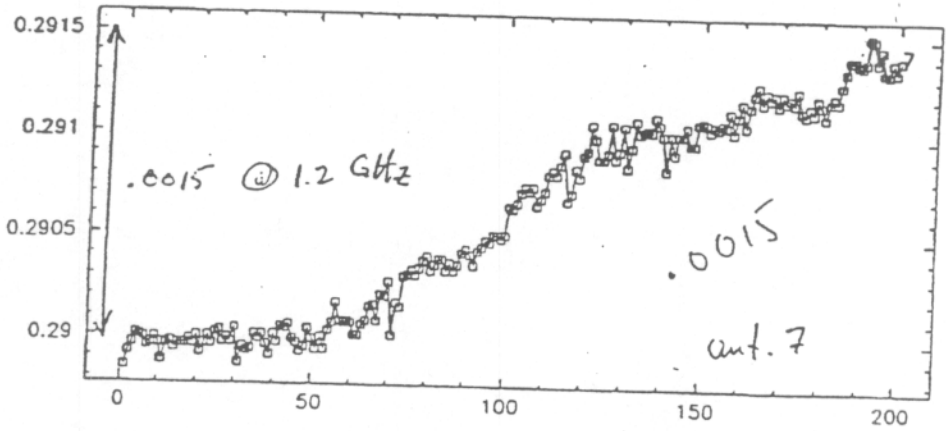

Fig 2 b

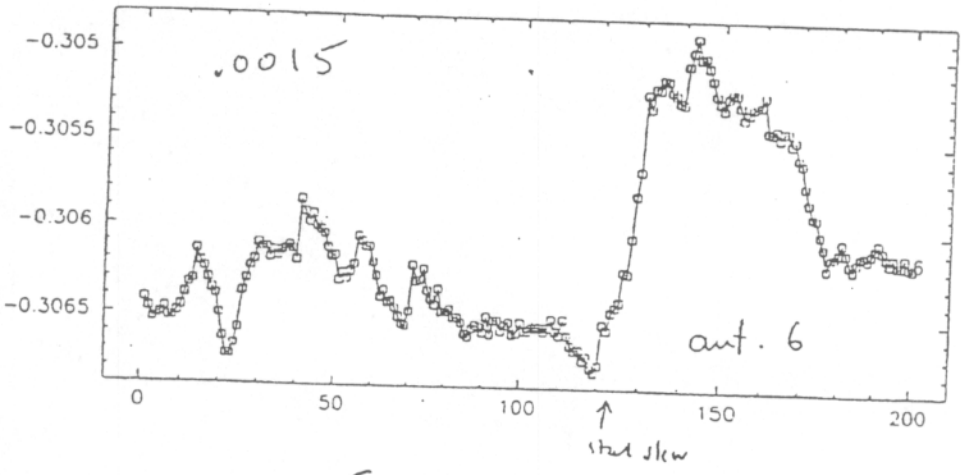

Fig 2c

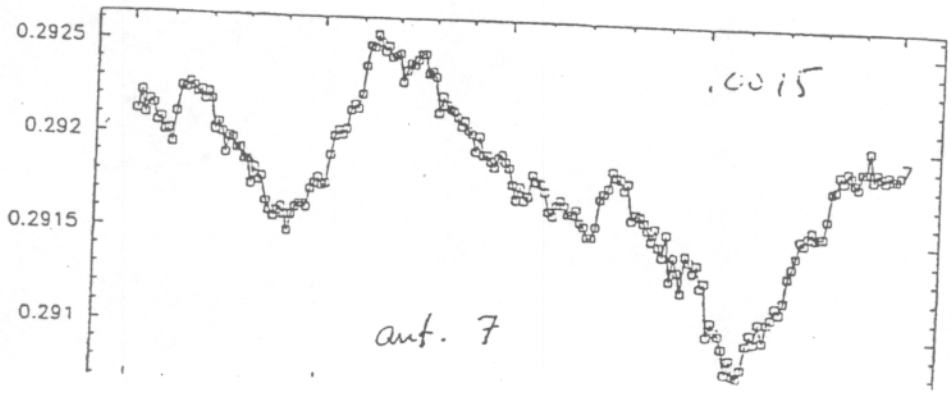

Fig 2d

(4)

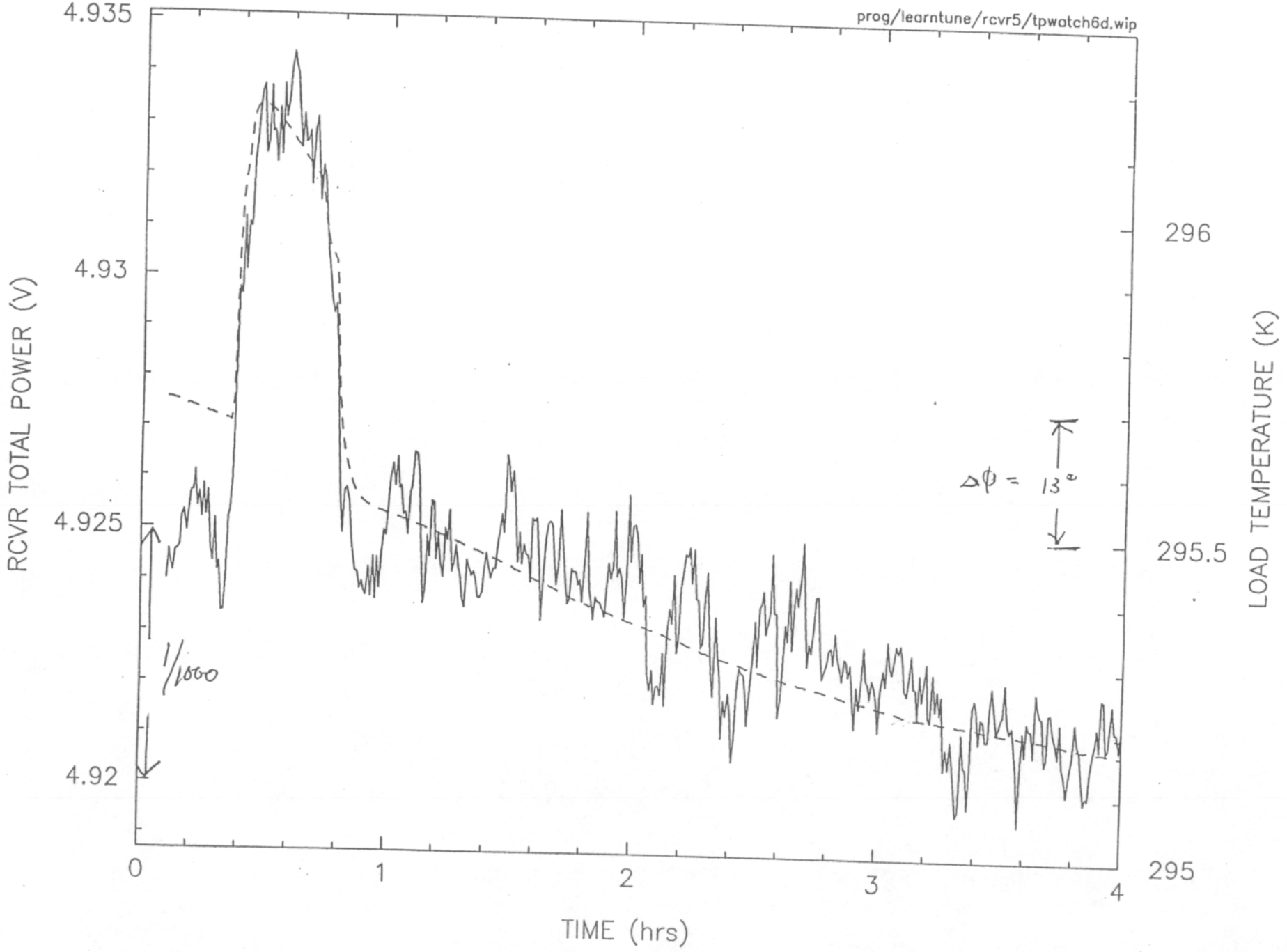
prog/learntune/rcvr5/tpwatch6d.wip
4.935
4.93
4.925
4.92
RCVR TOTAL POWER (V)
1/1000
0
1
2
3
4
TIME (hrs)
296
295.5
295
LOAD TEMPERATURE (K)
Δφ = 13°

Figure 3

IRAM

Stability of IRAM-30m receivers

B.Lazareff, 28-Mar-2001

The data were obtained in Oct/Nov 1998, during or shortly after commissioning of the first two of the four dual-frequency receivers of the new receiver cabin. Acquisition was by myself and S.Navarro, using software written by G.Paubert.

The total power of the four receivers was sampled in parallel at 20Hz, using the full IF bandwidth (0.5GHz for A100/B100, 1.0GHz for A230/B230), for a duration of 900sec, and for various frequency setups. The receivers were always tuned SSB, with signal in LSB.

All the data acquired is presented in the attached PostScript files, with the exception of those data obtained while debugging a faulty ambient IF amplifier.

Definition of stability.

The ALMA spec is 10^{-4} on timescale of 1s. That is not a precise definition. And, is 1sec really the relevant timescale for continuum observations for an antenna without a chopping secondary?

Definition of Allan variance

I used the following algorithm, maybe easier to follow in words:

- Choose a set of integration times τ_i, in roughly exponential progression between the sampling time τ_s and 1/8 of the duration of acquisition (poor statistics for largest values of τ); the choice of intermediate values is purely cosmetic.
- For each τ_i, compute: $\delta_k = \frac{1}{\tau}\left[\int_{k\tau}^{(k+1)\tau} s\,dt - \int_{(k+1)\tau}^{(k+2)\tau} s\,dt\right]$ where s is the measured total power, and k ranges from 0 to the largest value allowed by the size of the data set. Then compute the variance for timescale τ_i, as: $V_i = \frac{1}{2}\left\langle \delta^2 \right\rangle$; the $\frac{1}{2}$ factor is such that V is $\frac{1}{B\tau}$ for an ideal radiometric system.

Modified Allan variance

Same as above, except:

$\delta_k = \frac{1}{\tau}\left[-\int_{k\tau}^{(k+1)\tau} s\,dt + 2\int_{(k+1)\tau}^{(k+2)\tau} s\,dt - \int_{(k+2)\tau}^{(k+3)\tau} s\,dt\right]$, and the $\frac{1}{2}$ factor is now $\frac{1}{6}$, so that again, V is $\frac{1}{B\tau}$ for an ideal radiometric system.

Notes about the plots.

V(1sec) = 10^{-4} seems to be within reach, but is not routinely achieved. Two Allan plots for A230 and B230 reach variances well below 10^{-4} for 1sec timescale. The reason for this atypical behavior is not clear. In that case, both receivers were tuned for 260GHz sky freq, where their receiver noise performance is degraded by ~2x w/r to the band center.

The modified Allan variance is expected to remove the effect of linear drifts. The corresponding plots actually show only marginal improvement over those for the "straight" Allan variance.

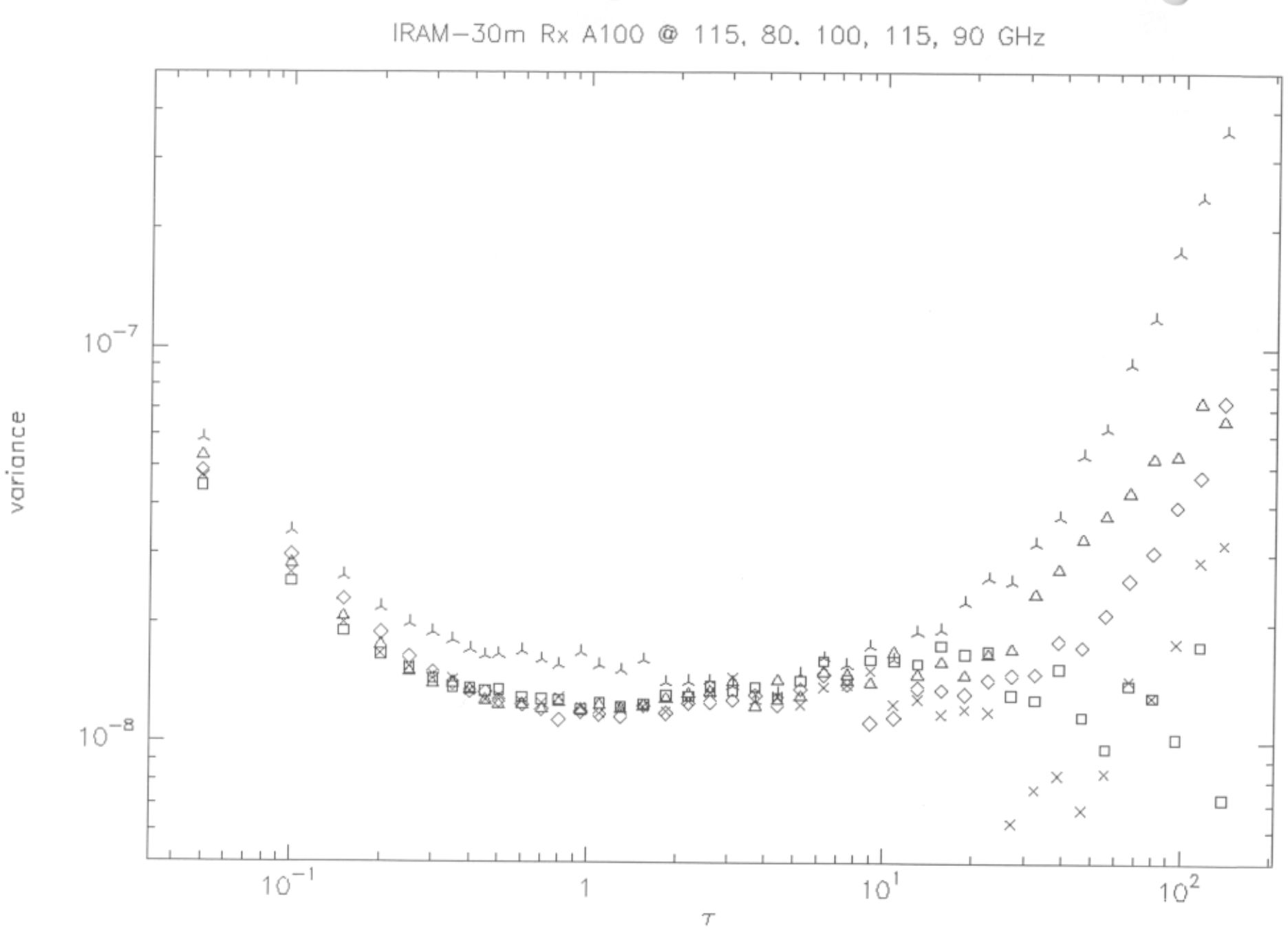
IRAM–30m Rx A100 @ 115, 80, 100, 115, 90 GHz
variance
10^{-7}
10^{-8}
10^{-1}
1
10^{1}
10^{2}
τ

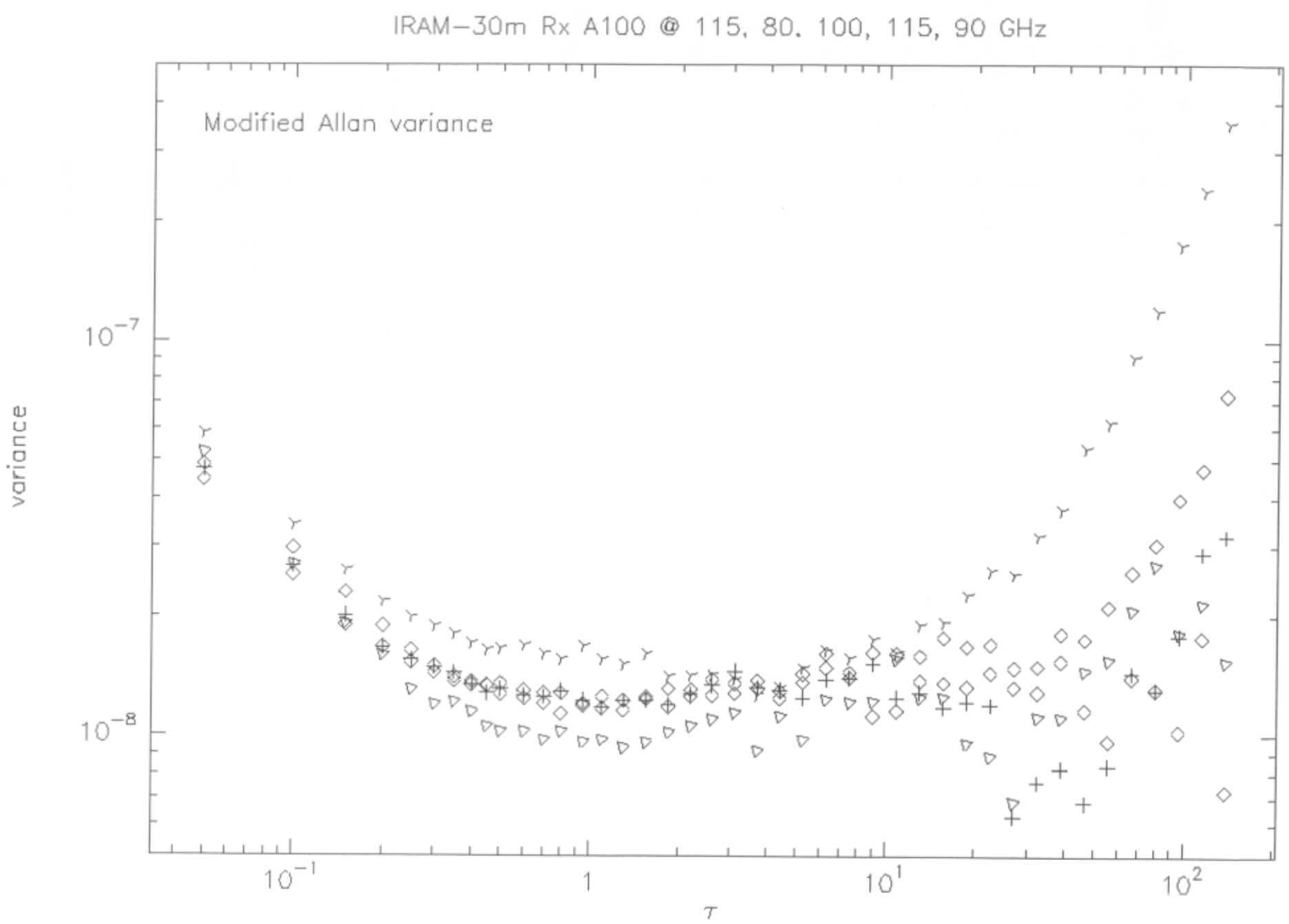
IRAM–30m Rx A100 @ 115, 80, 100, 115, 90 GHz
Modified Allan variance
variance
10^{-7}
10^{-8}
10^{-1}
1
10^{1}
10^{2}
τ

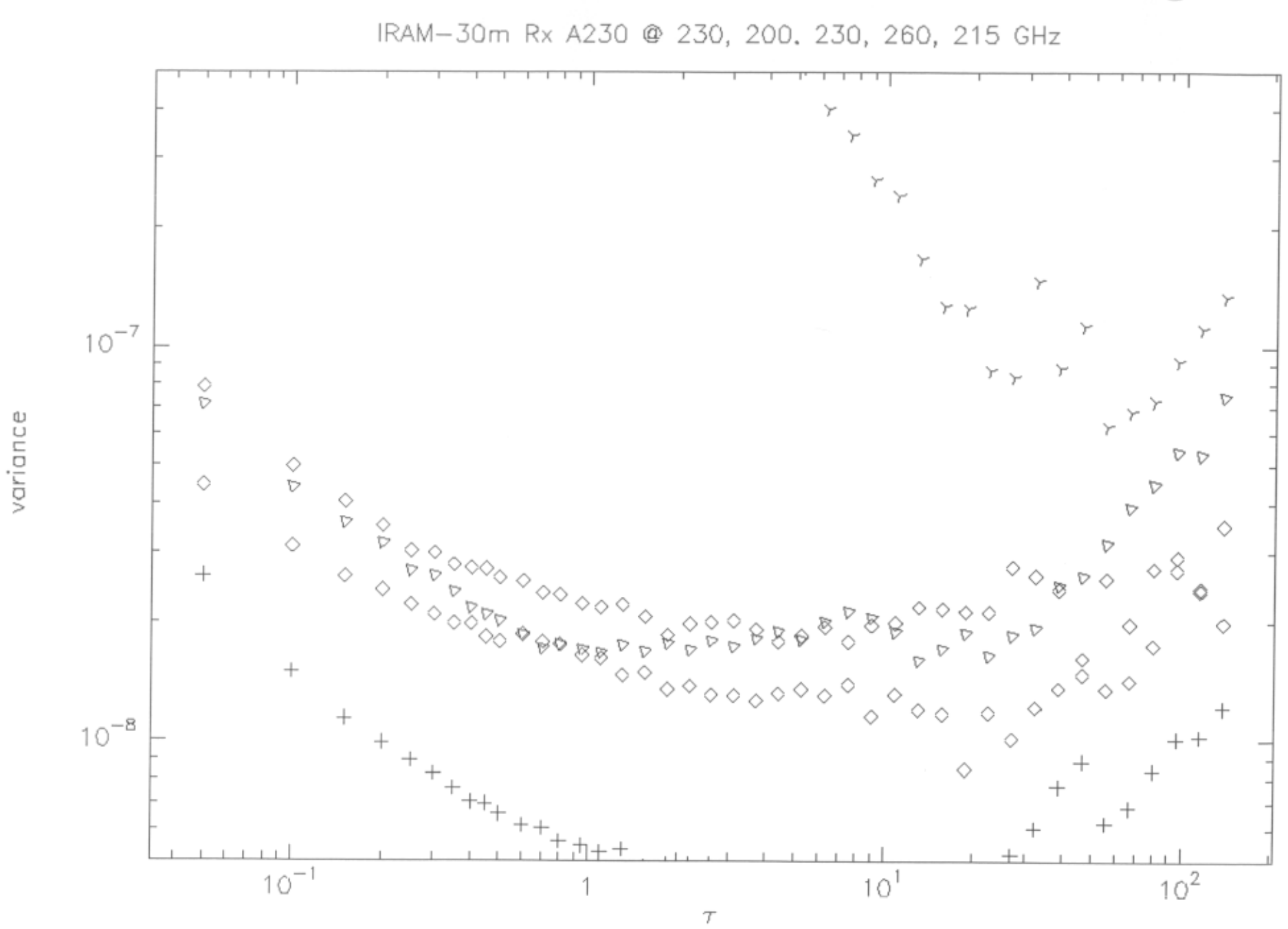
IRAM–30m Rx A230 @ 230, 200. 230, 260, 215 GHz
variance
10^{-7}
10^{-8}
10^{-1}
1
10^{1}
10^{2}
τ

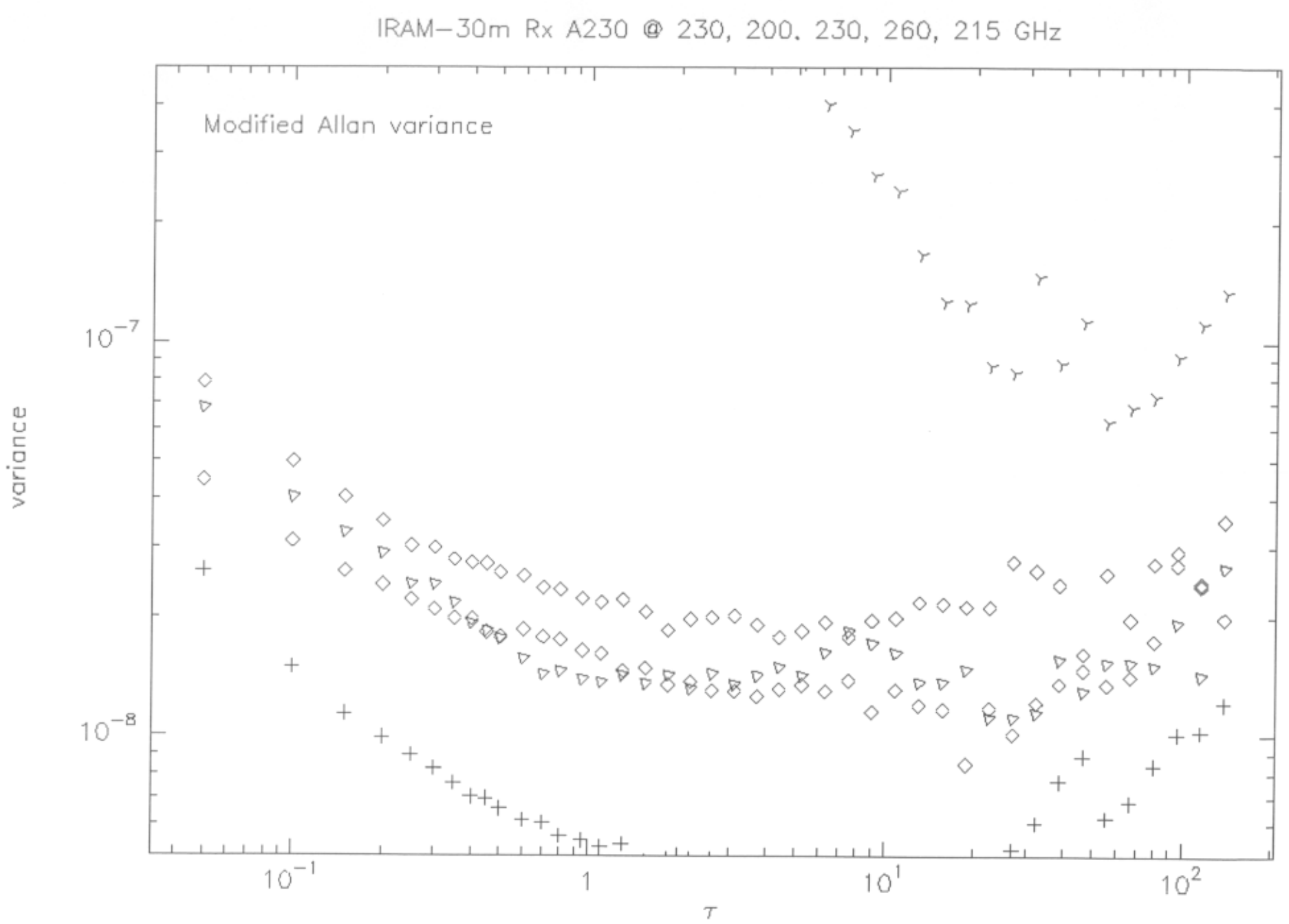
IRAM–30m Rx A230 @ 230, 200. 230, 260, 215 GHz
Modified Allan variance
variance
10^{-7}
10^{-8}
10^{-1}
1
10^{1}
10^{2}
τ

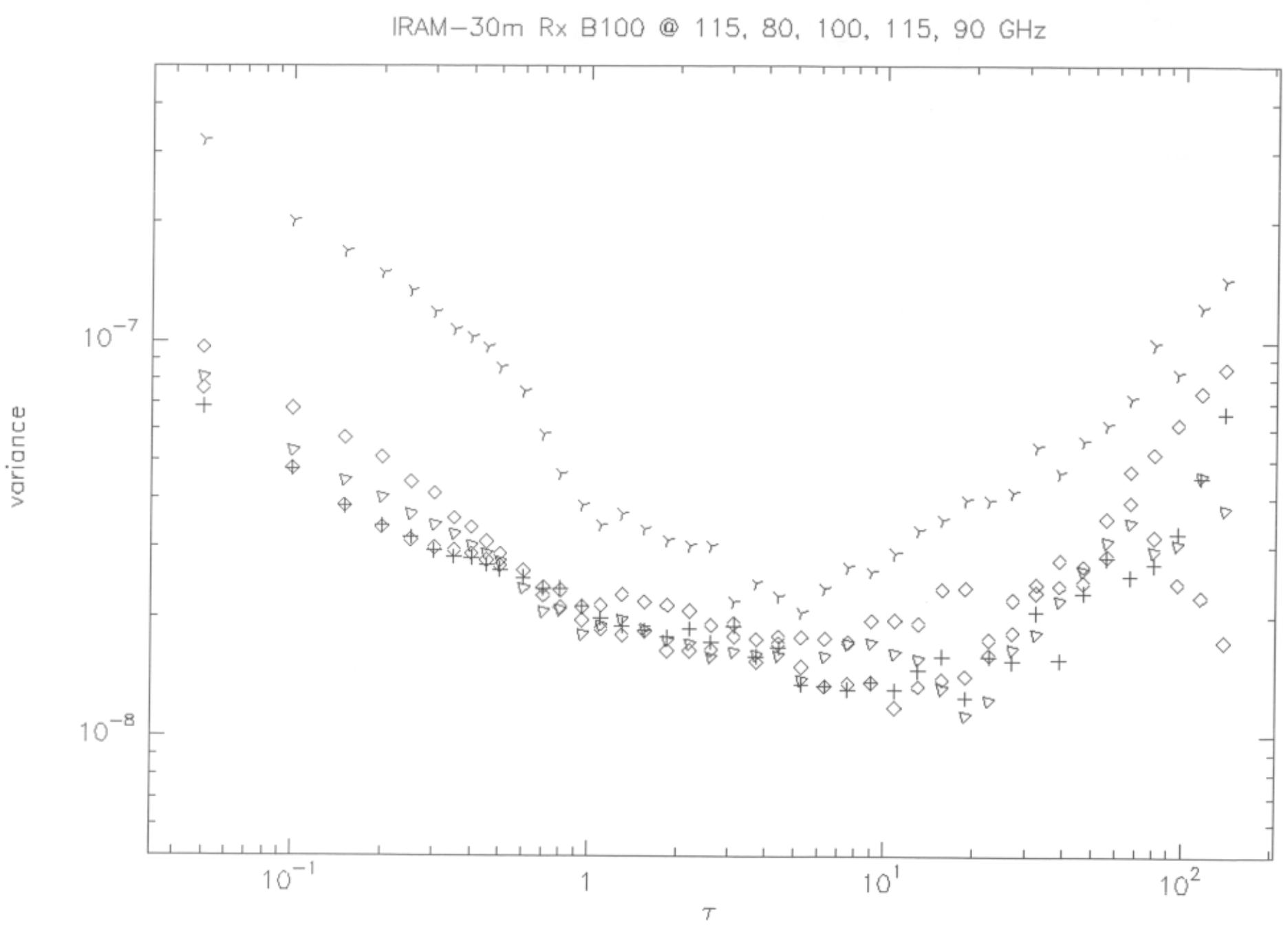
IRAM–30m Rx B100 @ 115, 80, 100, 115, 90 GHz
variance
10^{-7}
10^{-8}
10^{-1}
1
10^{1}
10^{2}
τ

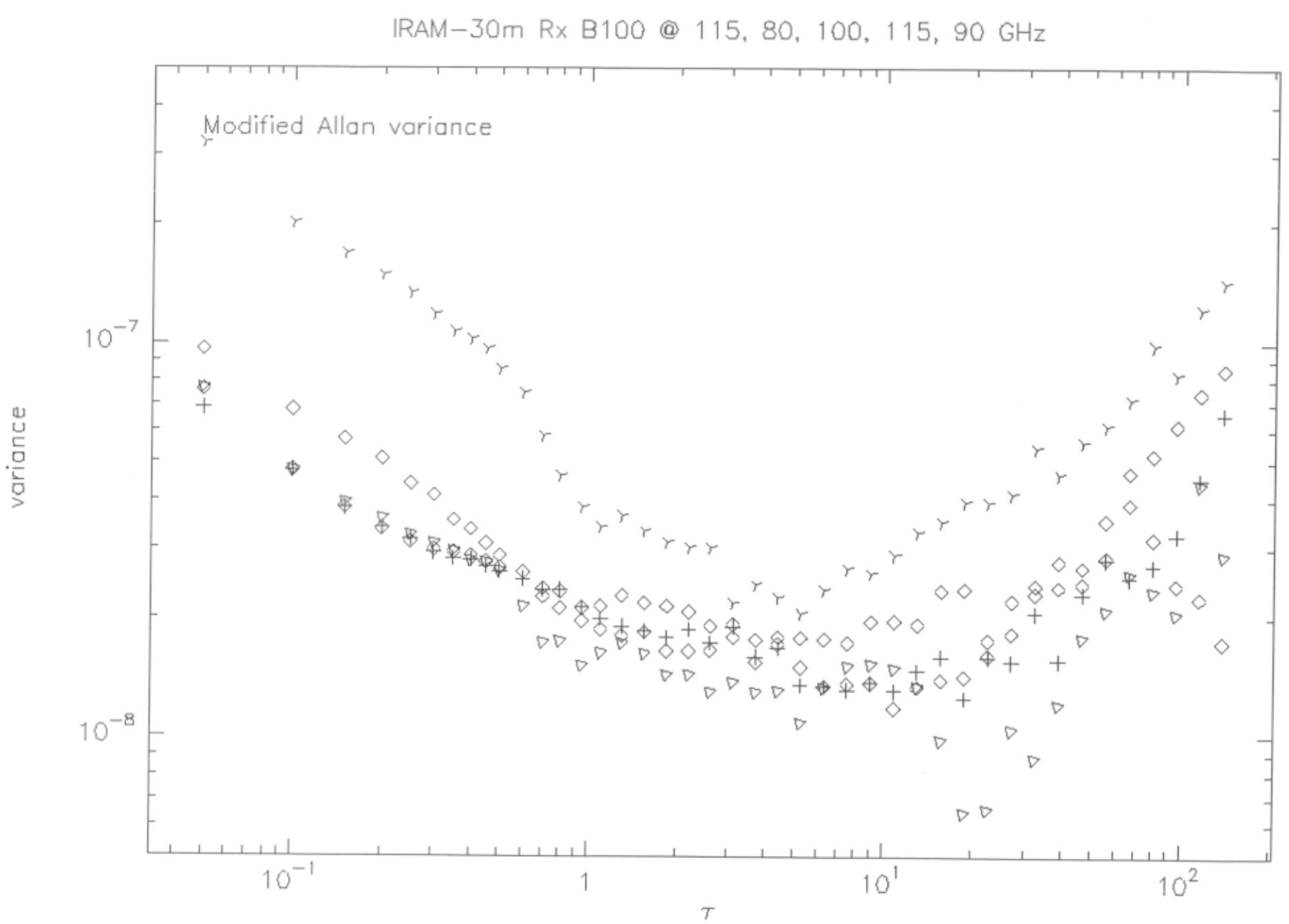
IRAM–30m Rx B100 @ 115, 80, 100, 115, 90 GHz
Modified Allan variance
variance
10^{-7}
10^{-8}
10^{-1}
1
10^{1}
10^{2}
τ

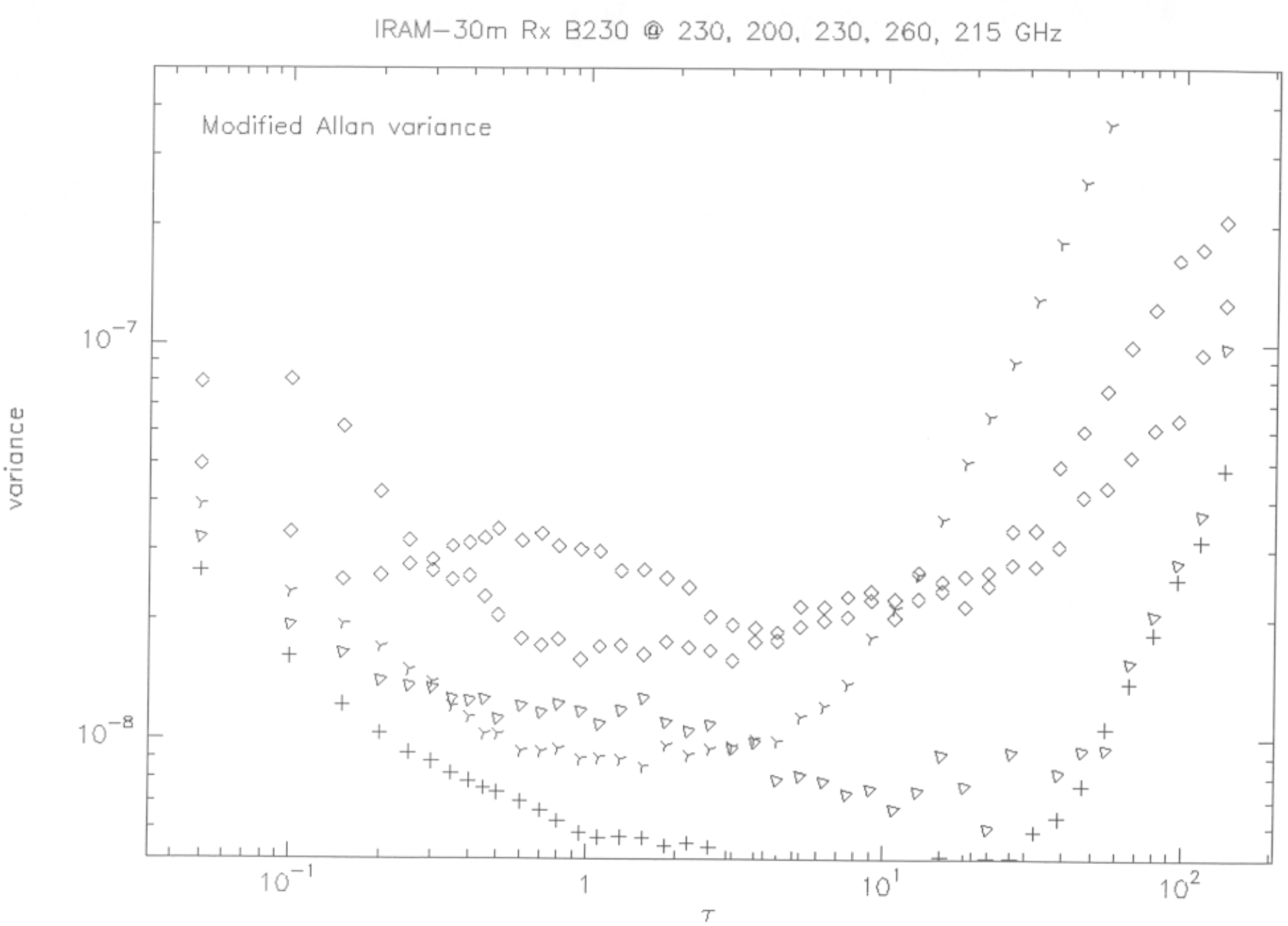
IRAM–30m Rx B230 @ 230, 200, 230, 260, 215 GHz
Modified Allan variance
variance
10^{-7}
10^{-8}
10^{-1}
1
10^{1}
10^{2}
τ

Pole STAR

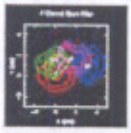

Lab Performance

Pole STAR Performance Measurements

We received the repaired 810 GHz local oscillator system from U. Mass last Friday (October 6). The LO works great and puts out 43 uW. Unlike most other 810 LO's, the multiplier is fixed tuned at our observing frequency and self-biased, making it ideal for polar operations.

When coupled through our quasi-optical LO power divider and Martin-Puplett diplexer, each of the four Cologne mixers receives sufficient LO power to conduct performance tests. Indeed, the LO power to 2 of the mixers must be attenuated to keep them from going into saturation.

Click here for a COOL image of a laser beam being diplexed by our quasi-optical LO power splitter. At optical wavelengths, the beams emerge with different intensities because of optical attenuation in the quartz "beamsplitters".

Figure P1: Repaired LO system installed on Pole STAR.

Click on thumbnail for full-size image!

Receiver Noise Measurements

Below are figures showing the LO pumped IV curves of each of the 4 mixers together with IF power sweeps. The red curve shows the IF power output when a HOT (290K) load is placed in front of the receiver. The blue curve shows the response with a COLD (77K) load . For receivers channels 1, 2, and 3 we obtain Y-factors of ~1.2. Channel 4 currently has a Y-factor of 1.12. It is most likely that we will need to direct more LO power to mixer 4 to get better performance. The LO beam for mixer 4 is the one most sensitive to alignment in our LO power splitter box. With a bit more adjusting of the optics, we feel confident we can get this Y-factor up to the level obtained with the other mixers. A Y-factor of 1.2 corresponds to a receiver noise temp of ~970K and includes all loss (optics, windows, filters, IF amp, etc.) in the system.

Screen shots were made of the receiver passbands on a spectrum analyzer under HOT and COLD load conditions. These are shown for receiver #2 in the "Total Power Stability" figures below. As with all the mixers, the receiver response is found to be constant across the 1 GHz IF passband.

Receiver stability was measured by monitoring the IF output power of 2 of the receivers over ~1000 sec. The IF power variation was well less than 1 percent over this period. Strip charts of these measurements are shown below.

It should be noted that all the above measurements were made with the SIS junctions biased in `resistive-mode'. Typically, junctions are biased to maintain a constant bias voltage. Our bias system has this ability and we are now making the small modifications needed to permit this mode of operation with the Cologne mixers. Even in resistive mode, the system is stable enough for observing on AST/RO.

I-V and hot-cold Total Power Curves

Click on thumbnails to view full-size images!

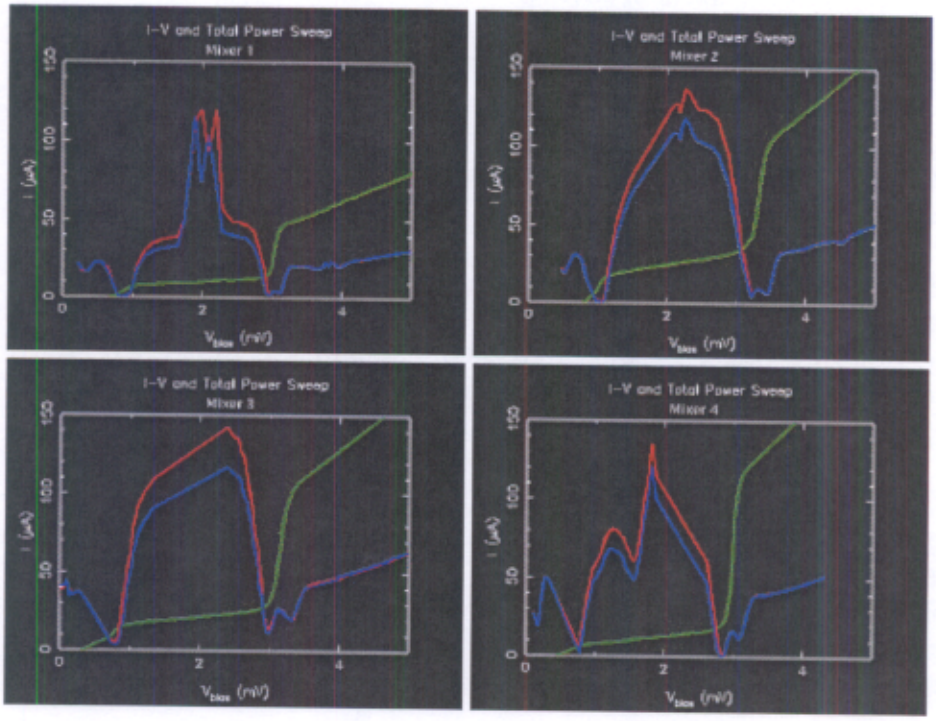

Total Power Stability Tests

Click on thumbnails to view full-size images!

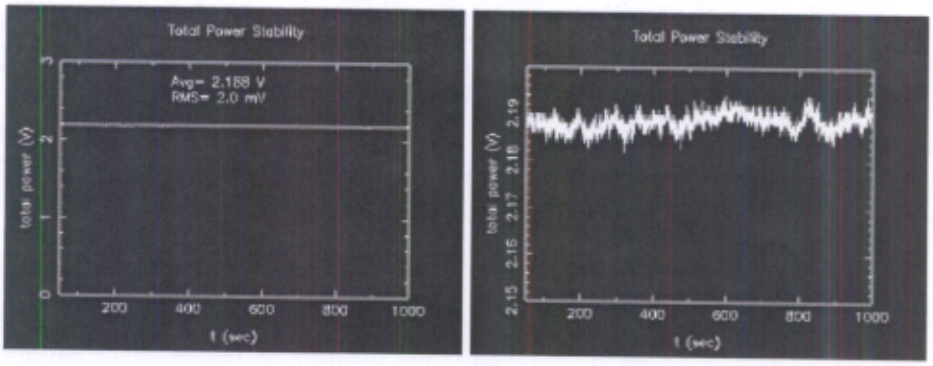

IF Passbands

These plots are on a LINEAR scale.

Click on thumbnails to view full-size images!

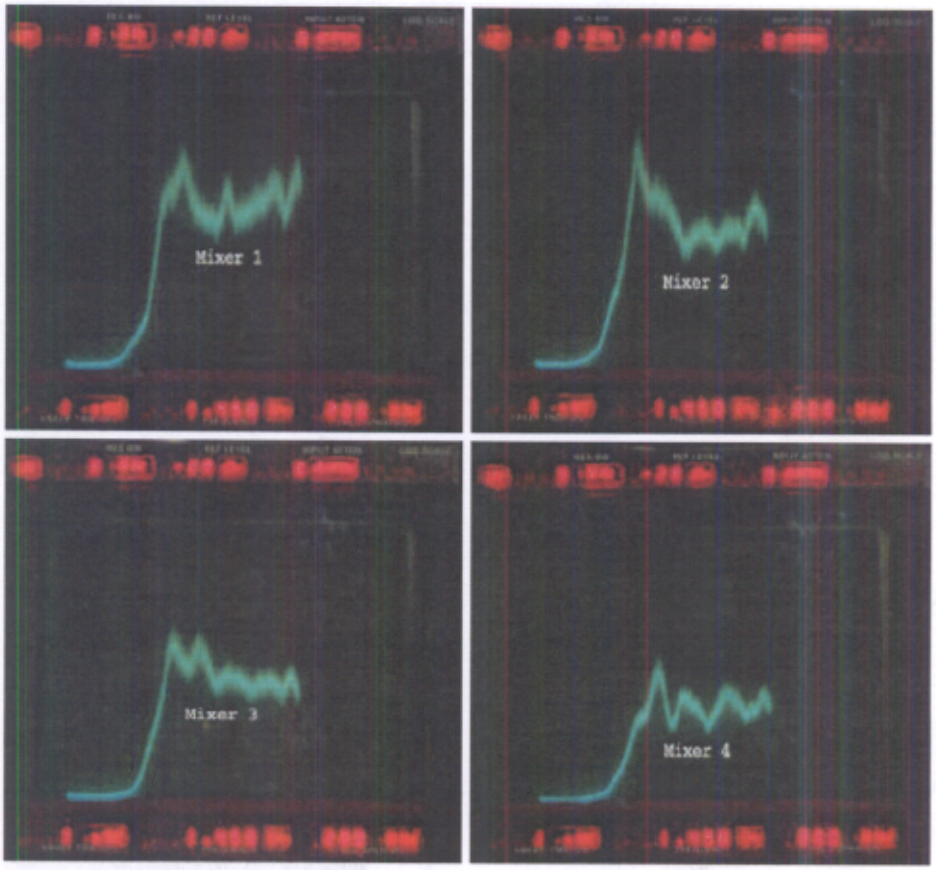

Hot-Cold Passband on Mixer 2

These plots are on a LINEAR scale.
Click on thumbnails to view full-size images!

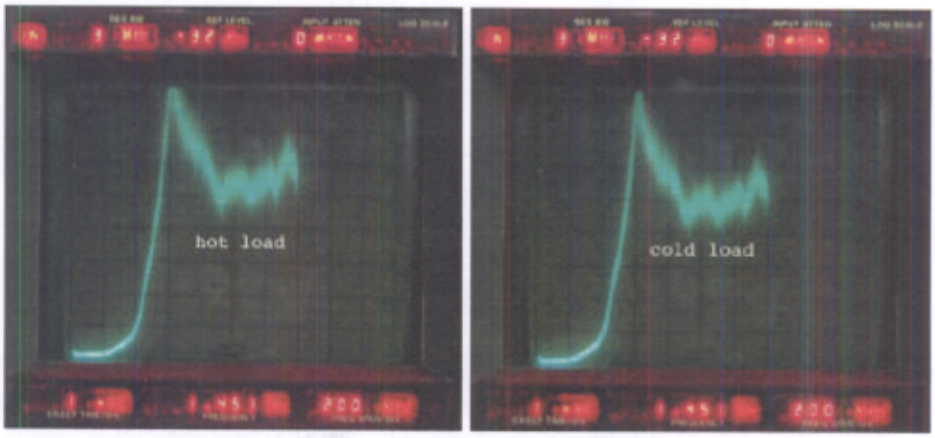

Low Frequency Spectrum Analyzer output of Mixer 2

These plots are on a relative LOG scale. The left plot covers the 0.1 to 10 Hz range, the right plot shows the 10 to 100 Hz range. All four receiver channels have been tested and show similar responses.

Click on thumbnails to view full-size images!

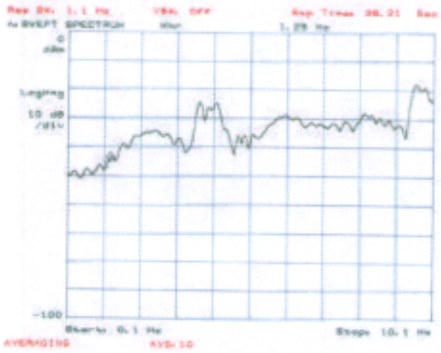

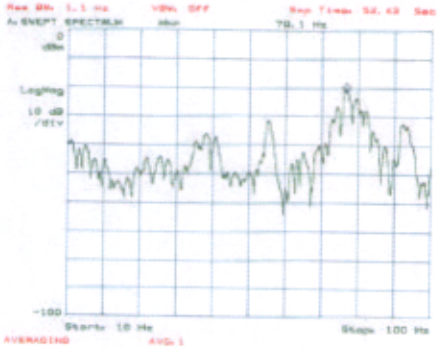

Beam Pattern Measurements

A computer controlled antenna test range (Figure P2, right) was constructed to measure the 4 Pole STAR beams. We used a liguid nitrogen load with a 3/8" aperture as the signal source. The signal was chopped and synchronously detected using a lock-in amplifier connected to the receivers' total power output. Maps of the 4-beams and their relative placement are shown below. To within the measurement errors the beams have the right size and shape. One beam (from Mixer 3) appears to have a squint angle compared to the others. This squint is probably due to a small mechanical misalignment of the mixer. Once the dewar is warm, we will try adjusting the mixer mount. Even with the squint, the Mixer 3 beam will clear all apertures on AST/RO and make it onto the sky.

Figure P2: Daedal X-Y stages used for beam measurements. The location of the X-Y stages is approximately at the distance of the azimuth bearing for AST/RO.

Click on thumbnail for full-size image!

Beam Measurements

The contour scaling is 12.5% per division on a LINEAR scale. The half power point is thusly the 4th contour from the peak.

Click on thumbnails to view full-size images!

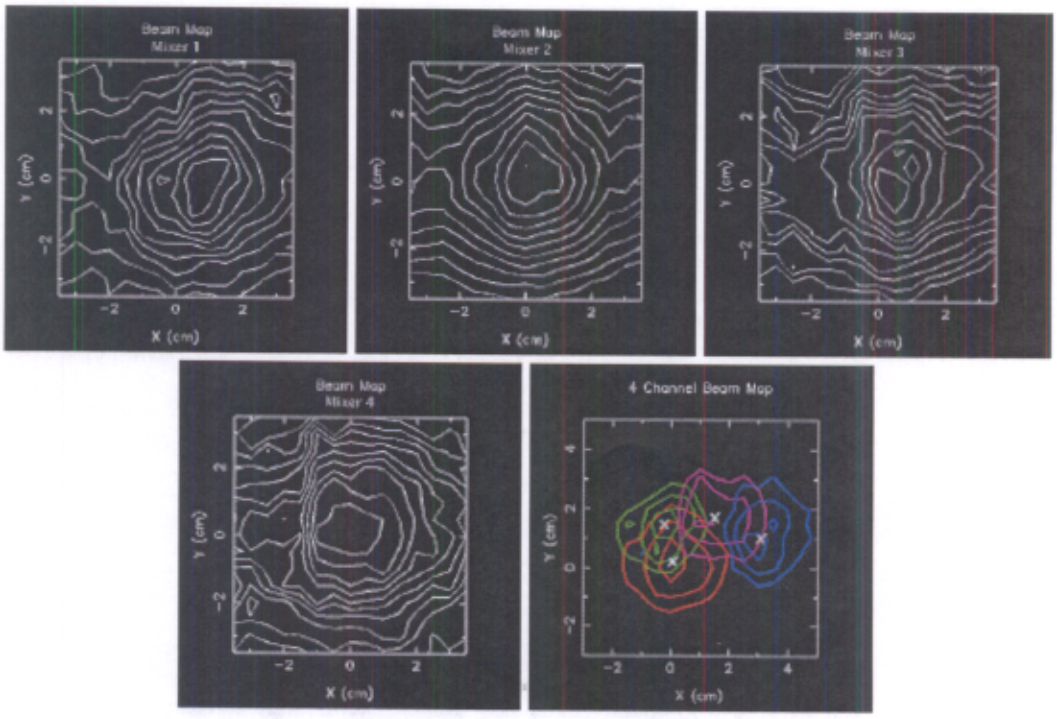

← Go back

Contact Chris Walker about Pole STAR performance

Last modified: Fri Oct 13 17:00:07 MST 2000

SEST

SEST - System Performance
Allan Variance

The gain stability is measured to find the maximum integration time inherit to the system (that is the spectrometers in combination with the receivers) for which the noise decreases (cf. A in Fig. below). After a short plateau, where the noise level stays stable (B), the noise will then start to increase (C) again due to system instabilities (flicker noise). However, under normal observing conditions, the sky noise level is above this system noise, thus longer integration times will be useful up to a given maximum integration time. Experience has shown this time to be no more than 240 seconds under perfect observing conditions.

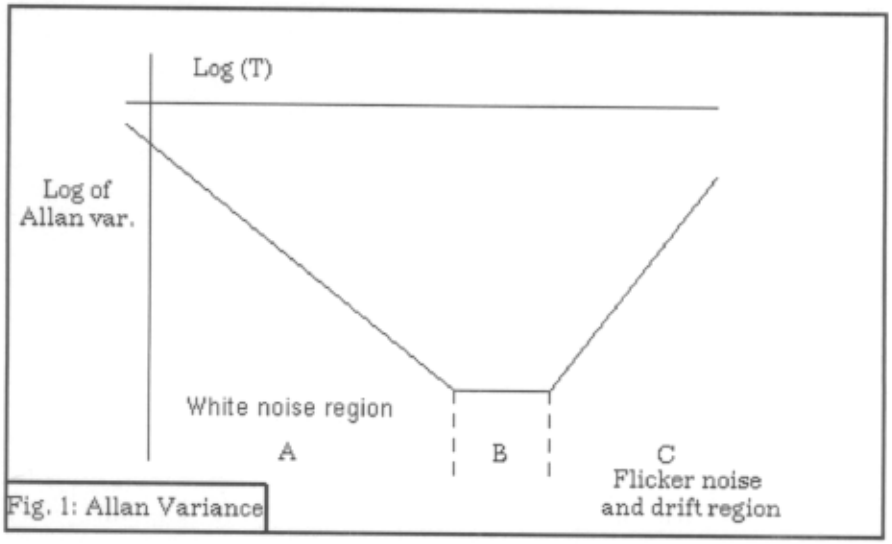

Fig. 1: Allan Variance

The gain stability is measured on only three of our spectral line receivers (RX100, RX150 and RX345) in combination with the HRS. The results indicate a maximum integration time of the order of 30 seconds for the 100 GHz and the 150 GHz receivers, and 10 seconds for the 345 GHz receiver. In the following table, the results for RX100, RX150 and RX345 are presented based on the last measurements during 1995. Measurements for RX115 and RX230 are expected to be available very soon:

Receiver	Frequency (GHz)	Maximum Integration Time [s]
RX100	86	25
RX115	n.a.	n.a.
RX150	147	29
RX230	n.a.	n.a.
RX345	345	11.5

Page updated by Felipe Mac-Auliffe, September 16th 2000
Send your comments, suggestions or questions to sest@eso.org

Kooi Paper

Noise Stability of SIS Receivers

J.W. Kooi, G. Chattopadhyay, M. Thielman, and T.G. Phillips

California Institute of Technology, 320-47, Pasadena, CA 91125, USA.

R. Schieder

University of Koln, Dept. of Physics.

Abstract

There is a strong interest in the submillimeter astronomy community to increase the IF bandwidth of SIS receivers in order to better facilitate broad spectral linewidth and continuum observations of extragalactic sources. However, with an increase in receiver IF bandwidth there is a decrease in the mixer stability. This in turn effects the integration efficiency and quality of the measurement. In order to better understand the noise mechanisms responsible for reducing the receiver stability, we employed a technique first described by D.W. Allan and later elaborated upon by Schieder *et. al.* In this paper we address a variety of factors that degrade the noise stability of SIS receivers. The goal of this exercise is to make recommendations aimed at maximizing SIS receiver stability.

Keywords

"Allan" Variance, SIS mixer stability, low noise amplifier, gain stability, bias noise, temperature fluctuation noise, acoustic vibrations, Josephson noise.

I. Introduction

RADIO astronomy receivers in general look at very weak signals deeply embedded in noise. To extract the weak signals, synchronous detection (signal on - signal off) is typically employed. This is done by either slewing the whole telescope back and forth so as to get the beam on/off the source, or by moving the secondary mirror (subreflector) of the telescope at a certain rate. The problem in both these cases is the dead time between observations, i.e., chopping efficiency.

A practical lower limit for slewing the whole telescope is typically 15 seconds, while chopping the secondary mirror can perhaps be as fast as 0.2 seconds (5 Hz). Frequency switching is possible and can be at a much higher rate, but suffers from a separate set of problems not discussed here.

If the noise in the receiver system is completely uncorrelated (white), it turns out that the rate of chopping (modulation frequency) has no effect on the final signal to noise ratio. This can be deduced from the well known radiometer equation (1) which states that the noise integrates down with the square root of integration time:

$$\sigma = \frac{< x(t) >}{\sqrt{(B * \tau_{int})}} \tag{1}$$

Here σ is the standard deviation (rms voltage) of the signal, $< x(t) >$ the signal mean, B the effective fluctuation bandwidth, and τ_{int} is the total integration time of the data set.

However, in practice the noise in radiometers, and in particular superconductor-insulator-superconductor (SIS) receivers, appears to be a combination of low frequency drift (correlated noise), 1/f electronic noise and white (uncorrelated) noise. Hence, there is an optimum integration time, known as the "Allan" stability time (T_A), after which observing efficiency is lost. In actual synchronous detection measurements "n" samples of difference data (signal on - signal off) are taken, each with a period T. These differences are then averaged so that the total observed time equals $n * (2T)$. If the period T is larger than the "Allan" stability time (T_A) of the system, then apart from loss in integration efficiency, there will be a problem with proper baseline subtraction. This manifests itself in baseline ripples at the output of the spectrometer which severely limits how well the noise integrates down with time.

In this paper an effort has been made to understand the de-stabilizing effects on a radiometer output due to:

• LNA bias noise and gain fluctuations of the cryogenic low noise amplifier immediately following the mixer.
• Temperature modulation of the SIS mixer and low noise amplifier.
• Acoustic noise pickup by the LNA and the local oscillator.
• Local oscillator pumping of the SIS mixer.
• SIS mixer bias noise and the effectiveness of suppressing the Josephson effect [5] by means of a magnetic field applied across the SIS junction.

The goal of this paper is to focus attention to the output noise stability of radiometers and SIS receivers in particular. This work is especially pertinent in light of the present trend to construct very large IF bandwidth SIS and HEB receivers for spectroscopic and continuum observations of very weak extragalactic sources.

II. Theoretical Considerations

To optimize observation efficiency, it is important to find the best secondary mirror (subreflector) chopping rate. This requires a knowledge of the nature of the receiver noise fluctuations. In practice, we have employed a method developed by Allan [2], Barnes [3], and further elaborated on by Schieder *et al.* [4].

Following Schieder's analyses of synchronous detection, two sets of contiguous data samples are taking, each with the same integration time (T). The first measurement is the signal s(t), and the second measurement is the off-source reference signal r(t). In the analysis, it is assumed that there is no dead time between the data samples. If we define the first measurement as:

$$S(T) = \int_0^T s(t)\ dt, \tag{2}$$

and the second measurement as:

$$R(T) = \int_T^{2T} r(t)\ dt, \tag{3}$$

then difference of the two measurements is

$$D(T) = S(T)\ -\ R(T). \tag{4}$$

Because we look at signals deeply embedded in the noise and are only interested in how the noise integrates down with time, we can make the simplification that there is essentially no signal present in s(t). This means that on average D(T) = 0, and s(t) = r(t).
If μ is defined as the mean of D(T) and σ^2 the variance of D(T) then

$$\sigma^2(T)\ =\ <[D(T)-\mu]^2>\ =\ <D(T)^2> - <D(T)>^2 \tag{5}$$

Here $<D(T)^2>$ is the mean (expectation value) of the difference squared and $<D(T)>^2$ is the squared mean of the difference. But since $<D(T)>$ equals zero we get

$$\sigma^2(T)\ =\ <[R_1(T)-R_2(T)]^2>\ . \tag{6}$$

From [2] we find that the "Allan" Variance is defined as:

$$\sigma_A^2(T)\ =\ 1/2\ \sigma^2(T) \tag{7}$$

The mathematical treatment of the above expression can be found in [3] for different types of noise spectra. If the noise spectral density is represented by a power law, then

$$S(f) = f^{-\alpha}, \quad \alpha = [-1, 3] \tag{8}$$

and one finds that

$$\sigma_A^2(T)\ \propto\ T^{\ \alpha-1} \tag{9}$$

where $\alpha = 0$ stands for white (uncorrelated) noise, $\alpha = 1$ for "1/f" noise, and $\alpha \geq 2$ for correlated low frequency (drift)

noise. Using a simple power law to characterize low frequency drift noise might not be correct. A more accurate representation would be to describe the noise by a correlation function, given by:

$$g(\tau) \;=\; < r(t) * r(t+\tau) > . \tag{10}$$

The "Allan" variance can then be expressed as:

$$\sigma_A^2(T) \;=\; \frac{1}{T^2}\int_{-T}^{T}(T-|\tau|)(g(\tau)-g(T+\tau))\;d\tau. \tag{11}$$

Because we are interested only in integration times less than the correlated (drift) noise time scale, the correlation function can be expanded in a power series with only a few terms:

$$g(\tau) \;=\; g(0) - a\tau^{\beta} \;\pm\; \ldots, \qquad \beta = 1, 2, ... \tag{12}$$

From equation (11) we get

$$\sigma_A^2(T) \;\propto\; T^{\beta}. \tag{13}$$

Combining equation (9) and equation (13) we find that for a noise spectrum that contains drift, white noise, and 1/f noise that the "Allan" variance takes the form:

$$\sigma_A^2(T) \;=\; aT^{\beta} + \frac{b}{T} + c, \tag{14}$$

where a, b, and c are appropriate constants. For short integration times, the variance decreases as $\frac{1}{T}$, as expected from the radiometer equation (1). For longer integration times, the drift will dominate as shown by the term aT^{β}. In that case, the variance starts to increase with a slope β which is experimentally found to be between 1 and 2. On certain occasions, it is observed that the variance plateaus at some constant level. This is attributed to the constant factor and is representative of flicker or 1/f noise in the electronics.

Plotting $\sigma_A^2(T)$ on a log-log plot demonstrates the usefulness of this approach in analyzing the radiometer noise statistics. For reference, a slope of $(\frac{1}{T})$ has been drawn in all figures. This represents the uncorrelated (white) noise part of the spectrum. The minima in the plot gives the "Allan" time (T_A), the crossover from white noise to 1/f or drift noise. For the sake of optimum integration efficiency, one is advised to keep the integration time well below the system's "Allan" time.

Finally, it is often of interest to estimate what happens to the "Allan" stability time if the IF bandwidth of the radiometer is increased. Solving equation (14) for T as a function of receiver IF bandwidth we get:

$$T_A \ \propto \ B_{IF}^{-(\frac{1}{\beta \ + \ 1})}, \qquad \beta = 1 - 2. \tag{15}$$

B_{IF} presents the IF bandwidth and β the slope of the drift noise as discussed above. As the uncorrelated (white) noise component of the mixer spectral output power is reduced, the intersect between radiometric (1) and drift noise (13) equations occurs at an earlier time. Where exactly the two curves intersect depends on the statistical nature of the long term drift. It should be noted that all data presented in this paper have been taken with a 100 MHz bandpass filter.

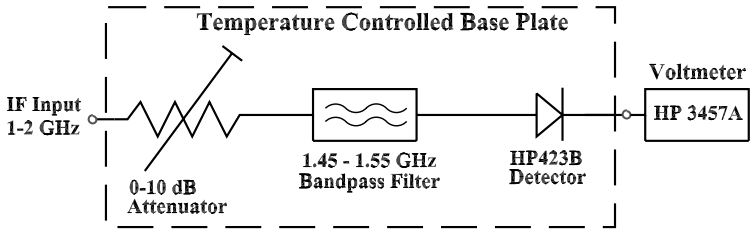

Fig. 1. Configuration of the "Allan" variance measurement setup. Unless otherwise stated, we have used a 50 mS sample time and 100 MHz bandwidth filter to acquire the data.

III. Measurement Setup and Calibration

The measurement configuration is shown in Fig. 1 and consists of a variable 0-10 dB step attenuator, a 100 MHz bandwidth filter, centered at 1.5 GHz, and a Schottky power detector. RF signal power on the detector has been kept constant to within 1 dB throughout the measurements. The whole unit is bolted to a 1 cm thick aluminum base plate and is thermally insulated from the surroundings. The output of the crystal diode is connected to a GPIB controlled 8.5 digit HP voltmeter. To test the stability of the system we ran a series of calibration tests such as the one shown in Fig. 2. The voltmeter is stable to at least 10 seconds, which turns out to be adequate for continuum noise stability measurements of SIS

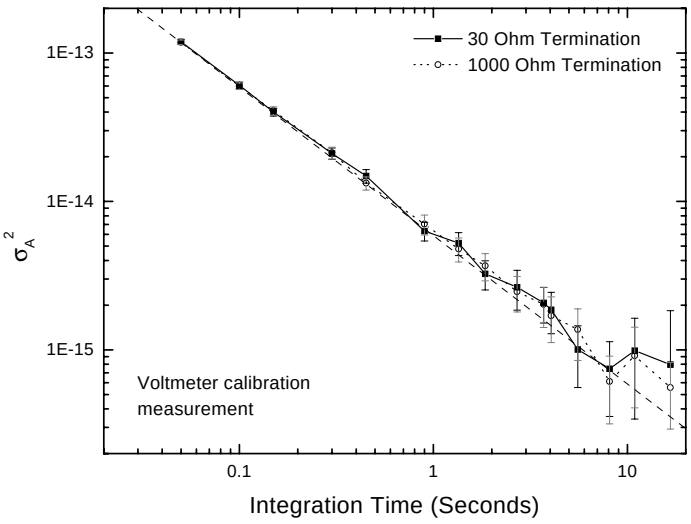

Fig. 2. HP 3457A Digital Voltmeter noise stability performance. The input to the voltmeter was terminated into 30 and 1000 Ohms. The two curves were taken several days apart, which indicates the stability of the measurement setup and HP voltmeter. The dashed line has a slope of 1/T.

receivers with IF passbands $\geq$ 100 MHz. All data presented in this paper is a statistical average of six 5 minute data runs, consecutive in time.

IV. IF Total Power box Stability Measurements

An IF total power box consists of a series of commercially purchased amplifiers, filters and couplers. The passband in use at the Caltech Submillimeter Observatory (CSO) is 1-2 GHz, and has an overall gain of 40-50 dB. With such a large gain, extreme precautions need to be taken to insure stable operation. The individual amplifiers are mounted on isolated pedestals which are heated to $\approx 45°C$. AC power is separated from the RF signal by different compartments inside the chassis. The chassis is built from thick aluminum

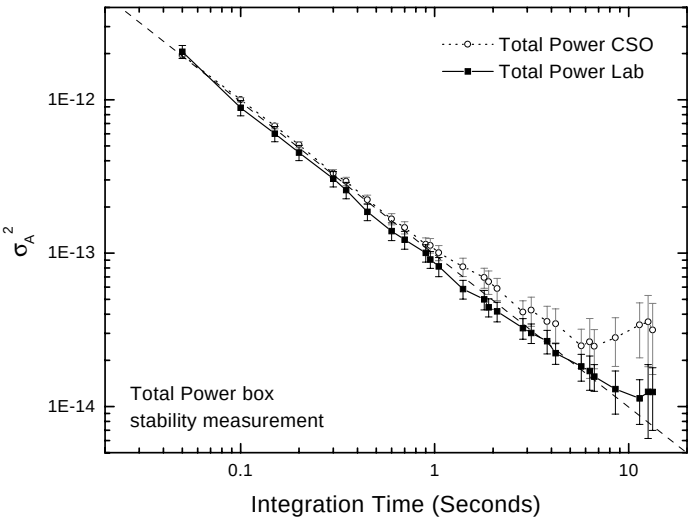

Fig. 3. IF Total Power box stability measurements in a 100 MHz bandwidth window at the Caltech Submillimeter Observatory (CSO) and in the laboratory. Note that the ambient EMI/RFI noise environment at the CSO is much higher than in the laboratory.

stock, which provides for a long thermal time constant.

In Fig. 3 we show the measured IF power box stability in the laboratory and at the CSO. The inputs to the total power box were terminated with a 50 Ω load. The IF power box at the CSO has a slightly shorter "Allan" variance time (≈ 7 seconds) than a similar IF power box in the laboratory (≈ 10 seconds). The difference is attributed to the much higher RFI and EMI noise environment at the observatory.

V. Low Noise Amplifier (LNA) Gain Fluctuations

Recently Schieder *et. al* have studied gain fluctuations of a 4-6 GHz cryogenic GaAs amplifier at both room and liquid helium (4.2K) temperatures with a Köln built Acousto Optical Spectrometer (AOS) [11]. The particular amplifier under discussion was built for the Submillimeter Array (SMA) project by the National Radio Astronomy Observatory [6]. The amplifier gain fluctuation, as measured differentially by subtracting two distinct AOS channels and integrating with time, was shown to be completely negligible when compared to the observed SIS receiver output noise fluctuation.

Schieder's measurements were performed with the amplifier mounted on the liquid helium stage of the cryostat. This however is different from the situation at many observatories. Frequently closed cycle helium expansion refrigerators are used in cryostats to reduce or eliminate the use of liquid helium. The refrigeration action vibrates the dewar, and may in fact produce small scale temperature fluctuations on the cryostat's temperature stages (usually 80K and 15K). Since the low noise amplifier (and sometimes even the mixer) is mounted to an active cooled stage, it is highly probable that acoustic vibrations and thermal fluctuations modulate the LNA and mixer, hence compromising the stability of the receiver.

To better understand the process, or mechanism, by which drift noise is introduced in the receiver a series of experiments were performed. These experiments use a 1-2 GHz balanced amplifier based on a design by Padin *et. al* [7] but adapted

by the authors to suit the needs of the CSO. This design uses GaAs Pseudomorphic HEMT devices very similar to those used in the NRAO 4-6 GHz amplifier in Schieder's experiment. For this reason it was felt not necessary to repeat Schieder's gain fluctuation measurements.

VI. LNA Bias Noise and Acoustic Pickup

We first mounted an amplifier with terminated input on the liquid helium stage of a passive cooled IR-Labs dewar [8] and compared the result against the same amplifier mounted on the liquid helium stage of an active cooled hybrid style cryostat [9][10]. The results are shown in Fig. 4. There appears to be little difference between the two dewars. Note that the

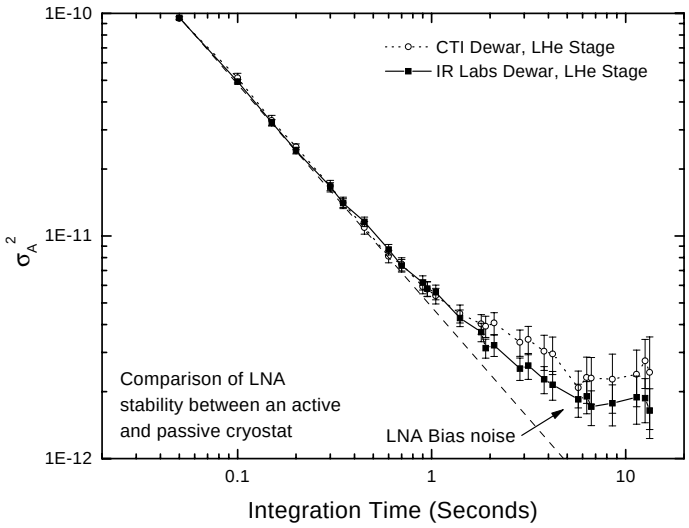

Fig. 4. Stability measurement of a low noise amplifier in an CTI cooled hybrid style dewar and a passive liquid helium cooled dewar. In both cases the amplifier is mounted directly to the 4.2 K liquid helium stage. The deviation from the 1/T slope (dashed line) is most likely due to low frequency noise on the amplifier bias line.

($\frac{1}{T}$) slope begins to deviate from the 100 % uncorrelated noise slope (equation 14) at about 1 second of integration time. The IF total power box stability measurement in the laboratory, shown in Fig. 3, does not deviate from the ($\frac{1}{T}$) slope until approximately 10 seconds however! The deviation from the ($\frac{1}{T}$) slope in Fig. 4 shows a loss of integration efficiency and is significant in that it indicates the presence of low frequency noise on the LNA bias line. This noise modulates the gate of the GaAs HEMT slightly thereby degrading the amplifier's long term noise stability. A resistive voltage divider network on the gate may provide the needed noise immunity. Note that the "Allan" time has only degraded slightly, from 10 to 8 seconds, as a result of the bias noise.

In the next experiment we transferred the balanced amplifier to the active cooled 15K stage of the hybrid cryostat,

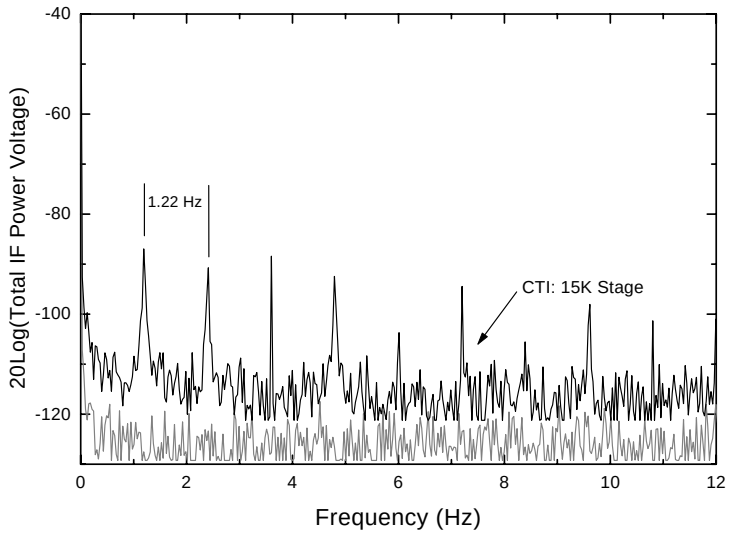

Fig. 5. Baseband spectrum of a low noise amplifier mounted on an active cooled (15K) stage and liquid helium (4.2K) stage. The two plots are offset to better show the difference.

everything else being the same. The amplifier low frequency baseband spectrum was observed by connecting a spectrum analyzer to the output of the crystal detector in Fig. 1. The baseband spectrum reveals the fundamental 1.2 Hz compressor action along with many harmonics (Fig. 5).

To find out whether harmonics are introduced acoustically or thermally, we remounted the amplifier on the liquid helium stage, but this time on four 1 cm long Teflon standoffs. This had the effect of vibration isolating the amplifier from the active cooled 15 K stage. The amplifier was then heat strapped to the 15 K stage with a 12 mm wide, 5 cm long, 2 mm thick copper strip. As can be seen in Fig. 6 the response

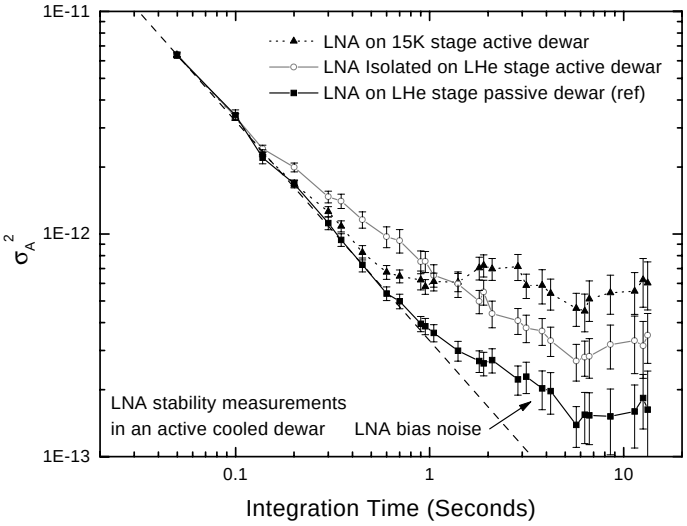

Fig. 6. LNA stability measurements with the amplifier mounted to the active cooled (15K) stage and to the liquid helium (4.2K) stage. In the latter case the amplifier was vibration isolated by mechanically connecting it to the LHe stage but thermally strapping it to the 15K active stage. The response in the case of a passive dewar has been included as a reference.

of the vibration isolated amplifier deviates rather quickly from the ($\frac{1}{T}$) slope (T_{int} = 0.1 Seconds). Presumably this is due to the not too ridged mount in our experiment, or perhaps a too solid connection (small mechanical time constant) to the active cooled stage. The overall improvement in integration time is seen to go from 0.8 seconds to 7 seconds if some loss in integration time efficiency is tolerated. This result can be improved upon with a more rigorous design however. The measured baseband spectrum in this case is shown as the bottom trace in Fig. 5. It is unclear what components in the amplifier, or wiring, are sensitive to mechanical vibrations. Presumably the result presented here will vary with different style amplifiers and mounting configurations. Nevertheless, it appears good practice that the LNA be vibration isolated by mounting it to the liquid helium stage, while at the same time be thermally connected to an actively cooled stage in the dewar to conserve helium. It is expected that at higher IF frequencies acoustic pickup will become less of an issue because amplifiers are more planar in design.

VII. LNA and SIS Mixer Temperature Fluctuations

Another means by which a radiometer's stability can be compromised is when the mixer and IF amplifier (LNA) are subjected to temperature fluctuations. A slow change in the physical temperature of the mixer, or amplifier, results in a change in receiver gain. Hence, temperature fluctuations manifest themselves as low frequency drift noise at the output of the receiver.

Because most, if not all, sensitive receivers utilize some kind of active cooling system, it is of interest to quantify the maximum allowed temperature drift given a certain "Allan" stability time. We assume an IF output signal of the form:

$$s(t) \;=\; s_o(1 + g_t t). \tag{16}$$

Here g_t is defined as the normalized drift in system gain, and s_o the nominal total power at t=0. Defining m_t as the slope

of the IF output drift with respect to time, it can be seen that $g_t = m_t/s_o$.
If we take two contiguous measurements, like the ones described by equation (2) and equation (3), and define

$$Z(T) = [S(T) \; - \; R(T)]/R(T) \; , \tag{17}$$

we obtain the variance of the relative drift:

$$\sigma^2(drift) \; = \; < [Z(T) - \mu]^2 > \; = \; < Z(T)^2 > - < Z(T) >^2 \; . \tag{18}$$

Since the mean of $Z(T) = 0$ (Section II), equation (18) simplifies to:

$$\sigma^2(drift) \; = \; < [(S(T) - R(T))/R(T)]^2 > \; = \; (g_t * T)^2 \; . \tag{19}$$

This corresponds to a $\beta = +2$ slope for the drift contribution in the "Allan" plot (equation (14)). At the same time we have for the radiometric noise (1)

$$\sigma^2(rf) \; = \; < [(S(T) - R(T))/R(T)]^2 > \; = \; \frac{2}{B * T} \; , \tag{20}$$

where B is the bandwidth and T is the integration time of the data sample.
From equation (7) and using the constant c to represent the 1/f electronic noise we have:

$$\sigma_A^2(T) \; = \; (g_t * T)^2 + \frac{2}{B * T} + c \; . \tag{21}$$

Differentiating with respect to T gives the "Allan" stability time minima:

$$T_A \; = \; (g_t^2 B)^{\frac{-1}{3}} \; . \tag{22}$$

Equation (22) can now be re-written so that given a desired "Allan" time we obtain an estimate for the maximum allowed rate of change in system gain:

$$g_t \;=\; ({T_A}^3 * B)^{\frac{-1}{2}} \;. \tag{23}$$

For example, if a radiometer requires a broadband total power continuum detection of 4 GHz and has a required "Allan" stability time of 1 second, we find a maximum allowed drift in system gain of $1.4 * 10^{-3}$ % per second (5.7% per hour).
Having calculated the allowed drift in gain, we can now get an idea of the maximum temperature fluctuation a SIS mixer and low noise cryogenic GaAs HEMT amplifier may be subjected to. Re-writing equation (16) in terms of temperature dependence gives:

$$s(t) \;=\; s_o(1 + g_T(T - T_o)) \;, \tag{24}$$

where g_T is defined as the normalized temperature dependent drift of the system. Let m_T be the slope (dP/dT), a property of the SIS mixer and amplifier, then $g_T = m_T/s_o$.
To obtain g_T for the 1-2 GHz balanced amplifier and LO pumped double slot SIS mixer [12], we performed the following experiments. First, the LNA was gradually heated from 4.2 Kelvin to 10 Kelvin in a time span of 1 hour (LNA input load at 4.2 Kelvin), while continuously recording the IF total power and amplifier physical temperature. In the second experiment we pumped a SIS mixer with LO power [12] and over the course of an hour varied it's temperature from 2.16 Kelvin to 9.6 Kelvin. The temperatures referred to in the text were measured at the outside of the mixer and amplifier block. During the LO pumped mixer experiment the LNA remained unheated at 2.16 Kelvin. g_T for both the mixer and low noise amplifier can be obtained directly from Fig. 7b. The SIS mixer has a negative temperature dependence, while the low noise amplifier has a positive and constant temperature dependence.

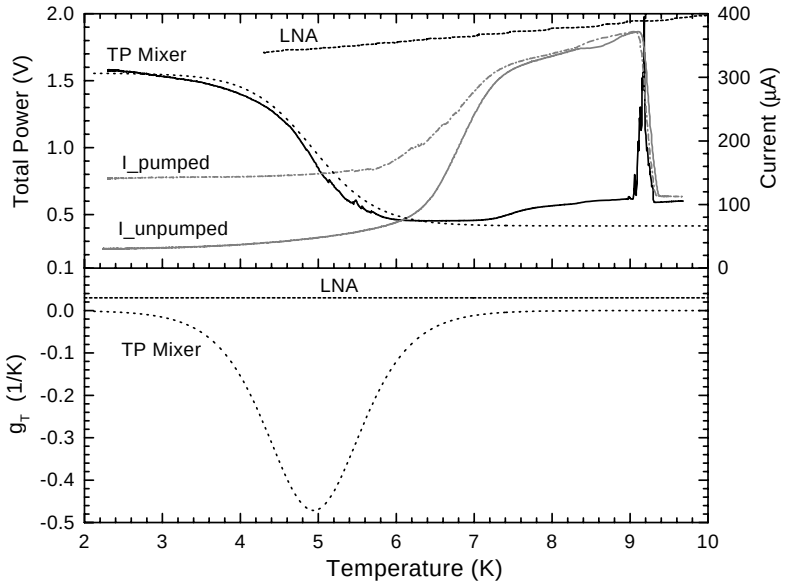

Fig. 7. SIS mixer and LNA gain sensitivity as a function of temperature. Note the large difference in sensitivity to temperature between the LNA and LO pumped SIS mixer. The pumped and unpumped SIS current has been included for reference. In the experiment the SIS junction was constant voltage biased at 2.2 mV, the peak of the total power response at 4.2 Kelvin. The computed normalized slope $g_T = (1/so * dP/dT)$ is shown in the bottom half of the figure and used in equation (25). Above 9.2 Kelvin the niobium film ceases to be a superconductor and the LO pumped junction current drops sharply.

As the physical temperature of the mixer in Fig. 7 is changed from 2.16K to 6K we see the mixer output noise drop in an exponential manner. The dotted line in Fig. 7a is a best fit Fermi function. As the temperature of the mixer block is increased from 2.16K to 6K only a minimal change in the junction's unpumped current (shot noise) is observed. The change in total power is to a very large extend caused by the temperature dependent conversion gain of the mixer. Above 7.2K we observe a jump in total power, which is attributed to

the by now large leakage current (shot noise) in the junction. At 9.2 Kelvin the niobium film ceases to be a superconductor and the LO pumped junction current drops sharply. Note, that the SIS mixer conversion gain sensitivity to temperature peaks around 4.9 Kelvin. This is unfortunately close to the 4.2 Kelvin bath temperature SIS mixers usually operate at (1 Bar atmospheric pressure). Moving to an high altitude site (600 mBar) improves the mixer conversion gain by $\approx$ 7-8% [14] and reduces the mixer's sensitivity to temperature fluctuations. Reducing the helium bath temperature to 1.5K would reduce this to a minimum.
Combining equations (16) and (24) we obtain the maximum allowed temperature change:

$$\delta T = t * \frac{g_t}{g_T} \tag{25}$$

g_t is obtained from equation (23) and g_T can be obtained from Fig. 7(b).

In the example of the 4 GHz bandwidth total power continuum detection (worst case senario) we estimate a maximum allowed gain drift of $14 * 10^{-4}$ % per second given a 1 second "Allan" time. At 4.2 Kelvin this gain drift equates to an allowed temperature drift of 470 μK/second for the LNA and 66 μK/second for the LO pumped SIS mixer! In high resolution spectrometer mode with a channel bandwidth of 100 KHz, 1 second of "Allan" stability time and an high altitude Helium bath temperature of 3.6 Kelvin, we find a maximum temperature fluctuation of 106 mK/second for the LNA and 48 mK/second for the SIS mixer (13.8 mK/second at 4.2 Kelvin bath temperature).

VIII. Receiver Stability with an SIS junction biased above the energy gap

In addition to acoustic, bias, and thermal noise pickup by the low noise amplifier, there is also a chance that the SIS receiver stability is compromised by low level noise on the mixer bias line. When we bias a SIS junction in the resistive

region above the superconducting energy gap (for niobium $\frac{2\Delta}{e}$ = 2.8 mV) we eliminate gain variation effects, since the mixer has zero gain.

Thus by comparing "Allan" variance stability plots of the LNA (Fig. 4) with "Allan" variance plots of the SIS mixer biased above the gap (Fig. 8) we study the effect of mixer bias fluctuation noise. The laboratory measurements described in this paper were taken with a 550 GHz dual-polarization SIS mixer [12]. The experiments described were taken under the following conditions:

- LNA mounted in a passive, IR-Lab, liquid helium dewar (ideal).
- LNA mounted to the LHe stage of an active cooled hybrid dewar.
- LNA mounted to the 15K stage of an active cooled hybrid dewar.

In the passive cooled dewar, we observe that the mixer output noise integrates down for roughly 10 seconds (bottom curve, Fig. 8). The manner in which the noise integrates down turns out to be nearly identical (within the error-bars) to the LNA noise, as shown in Fig. 4. The deviation from the $\frac{1}{T}$ slope at 1 second in Fig. 8 is clearly due to the LNA and not the SIS mixer. This experiment shows that the mixer is less susceptible to bias noise than the LNA. Presumably this is because of the much larger gain (30 dB vs -3dB in the case of the mixer) of the low noise amplifier.

The center curve in Fig. 8 shows both LNA and SIS mixer mounted to the LHe stage of the active hybrid style dewar. The top curve is for the case when the LNA is moved onto the active cooled 15K stage. In both these situations we see a consistent bump at 0.3 seconds. This effect has not been seen in measurements of the LNA alone, and is attributed to acoustic (CTI compressor harmonic) noise pickup on the mixer bias line inside the active cryostat. To verify this theory Schieder *et. al* ran simulations with Lorentzian shaped pulses on top of a white noise power spectrum. The amplitude of

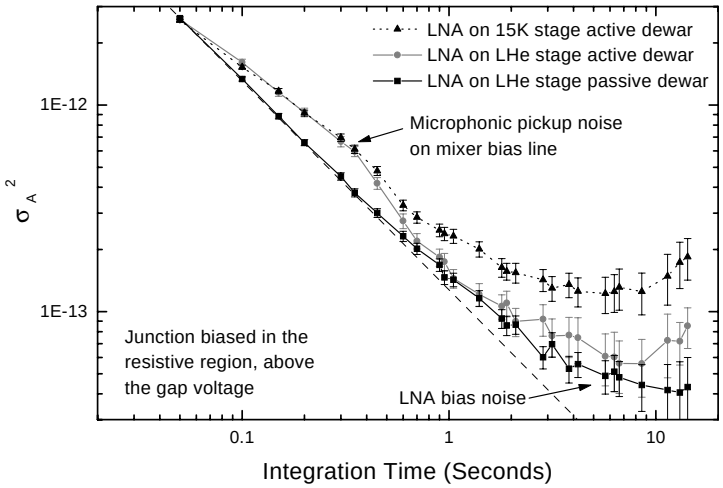

Fig. 8. Dual polarized cross-slot SIS mixer biased above the gap (5 mV). Mixer and low noise amplifier were mounted in a liquid helium (passive) dewar, and CTI cooled hybrid (active) dewar. In the hybrid dewar, the LNA was mounted two ways; directly onto the 15K active cooled stage and to the LHe stage.

these pulses was only 0.15 % of the mean data, practically invisible in the primary data set. His computer simulations indicate that the location and the shape of the bump does not depend very much on the repetition frequency but on the details of the structure of the pulses. Using these simulations we are able to closely match the experimental data and confirm the that the bump is indeed due to acoustic pickup induced by the refrigeration action of the hybrid dewar.

The SIS mixer bias circuit used in the experiments consists of a resistive bias network with $\sim$ 35 dB of noise isolation. Even so we see the effect of microphonic noise, which is consistent with Schieder's impulse response simulations. Note that the "Allan" variance stability time for a SIS-mixer/LNA

combination mounted to the LHe stage of the passive dewar and active cooled hybrid dewar is practically the same (bottom and middle curve, Fig. 8). This demonstrates that the interference noise does integrate down with time, though not as efficiently as one may like. In both these cases we measure an "Allan" time of roughly 8-9 seconds. This demonstrates that stable receiver operation with an active cooled cryostat is possible, with proper care and precautions.

As discussed, in the third experiment we moved the LNA (active cooled dewar) from the LHe stage to the active cooled 15K stage, keeping everything else the same. It is instructive to observe the drastic reduction in integration efficiency and "Allan" variance time (top curve, Fig. 8) due to acoustic vibrations of the low noise amplifier.

IX. Receiver Stability with the SIS mixer Biased in open and Closed Feedback Loop Mode

We have studied the receiver stability with the SIS junction biased above the gap in both "open' and "closed" loop voltage bias modes. Open loop is without bias feedback, while closed loop uses feedback to keep the voltage on the junction fixed. In the laboratory measurements discussed in section VIII we did not observe a difference between open and closed feedback bias methods. This is in contrast to the data taken at the CSO with a 345 GHz waveguide receiver [13], shown in Fig. 9. At the CSO the "Allan" variance time is a factor of two better without the voltage feedback than with the voltage feedback bias. We believe that this is due to the much higher ambient noise background at the observatory compared to the laboratory environment. The observatory is essentially a near perfect Faraday cage, with all the noise generated on the inside. The reference signal for the closed loop voltage is derived inside a SIS bias box, external to the dewar. Although the feedback loop bandwidth is only 80 Hz and the SIS bias circuit provides more than 40 dB of isolation, EMI noise is evidently still present on the SIS junction. It is expected that reducing

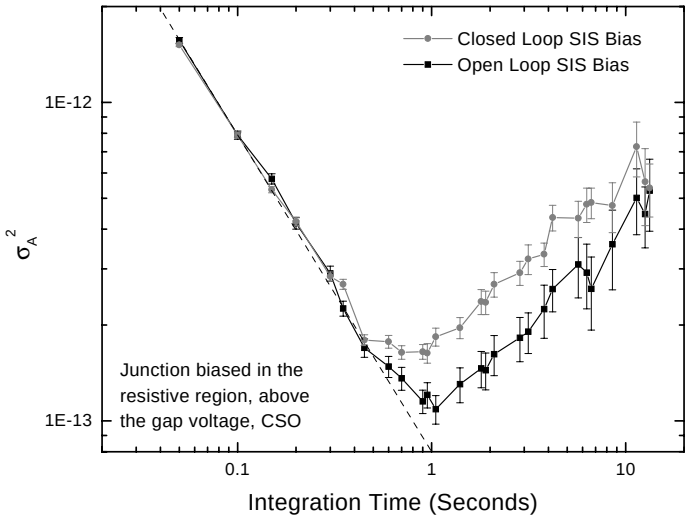

Fig. 9. 345 GHz receiver stability with the mixer biased at 5mV. No LO power was applied. "Allan" stability times are 1 and 2 seconds respectively for the open and closed voltage feedback bias configurations. The LNA is mounted on a 15K actively cooled stage. Data was taken at the Caltech Submillimeter Observatory.

the loop bandwidth will filter some of the noise, though not all. As a precaution, it may therefore be advisable to have a SIS junction bias source with two loop bandwidth's. One for tuning the mixer (fast time constant) and the other for observation mode (slow time constant). It should be noted that the receiver used in Fig. 9 has the amplifier mounted directly on a 15K actively cooled stage. We are currently investigating means of isolating the LNA from vibrations.

X. Receiver Stability with a 460 GHz LO Pumped SIS Junction

In Fig. 10 we show the effect of acoustic vibrations on a local oscillator (LO) pumped SIS mixer [12]. In all of the ex-

periments, great care has been taken to null out the Josephson oscillations in the junction [5]. The measurements were taken under the same conditions as in Section VIII.

Under the ideal condition of a passive cooled cryostat, we see that the noise integrates down nearly perfectly to 6 seconds. When we compare this result with the 9–10 seconds unpumped "Allan" variance time from the measurements with the junction biased above the gap voltage (Fig. 8), it is suggestive that Josephson noise in the superconducting junction, or bias noise induced gain variation, is limiting the receiver

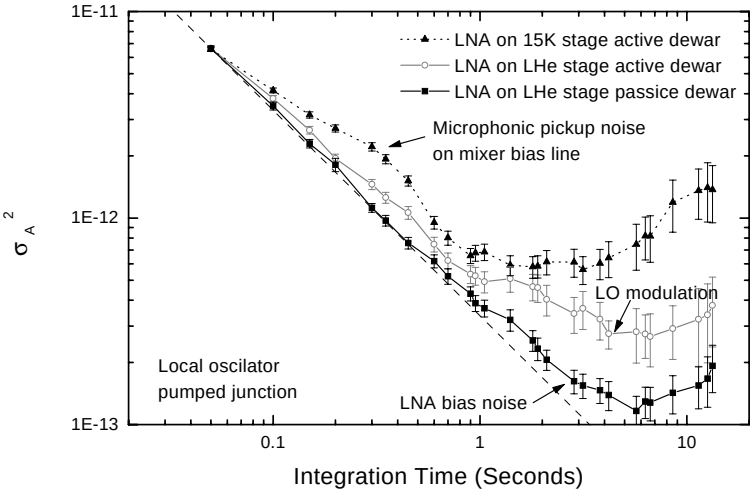

Fig. 10. LO Pumped cross slot with Josephson currents nulled out. The IF low noise amplifier was mounted in a IR-Lab liquid helium dewar, and CTI cooled hybrid dewar. In the hybrid dewar the LNA was mounted in two ways; directly to the 15K actively cooled stage and to the LHe stage. In the passive dewar Josephson instability, or SIS bias noise induced gain instability, shows up at 6 seconds! In the active hybrid dewar acoustic LO modulation becomes apparent for integration times between 1 and 6 seconds.

stability time. Note also that the slight deviation (bottom curve, Fig. 10) from the $\frac{1}{T}$ slope is once again due to the LNA bias noise (see Fig. 4). We used a free running Gunn oscillator followed by a quadrupler to pump the mixer. The whole assembly was mechanically disconnected from the passive cooled dewar. Ample time was given for the local oscillator unit to reach thermal equilibrium. The LO was injected quasi-optically by means of a 12 μm beamsplitter mounted to the side of the dewar.

Next, we changed from the passive dewar to the active cooled hybrid cryostat [9]. The LNA was mounted to the liquid helium stage of the hybrid dewar. The 460 GHz local oscillator chain and LO injection beamsplitter were physically attached to the side of the dewar, and were thereby subjected to the mechanical vibrations of the dewar. The result is shown in Fig. 10, center curve. Not only has the "Allan" variance time of the receiver degraded from 6 seconds to $\approx$ 4 seconds, but the "Allan" variance also begins to significantly deviate from the ideal $\frac{1}{T}$ slope at approximately 1 second. The CTI compressor has a 1.2 Hz cycle, and it is hypothesized that the local oscillator and beamsplitter are modulated at a harmonic of the cryo-cooling cycle.

Finally, when we mount the LNA at the 15K stage, we observe a further decrease in "Allan" variance time to 1.5 seconds. In this experiment we observe the net effect of acoustic vibrations of the LNA, micro-phonic noise on the LNA and SIS-mixer bias lines, mechanical vibrations of the LO chain (including beamsplitter), and Josephson noise suppression in the junction. This combined effect is in very good agreement to what has been measured at the observatory (Fig. 9). Loss in integration efficiency is now observed to occur at just 0.1 seconds.

Fig. 11 shows the effect of Josephson oscillations on the mixer stability. With the magnetic field (used to suppress Josephson currents) switched off, the "Allan" variance stability time of the receiver was reduced to a mere 0.8 seconds.

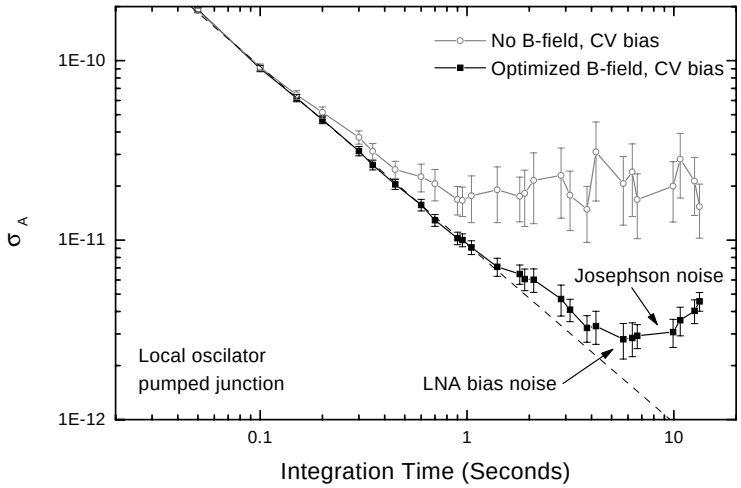

Fig. 11. LO Pumped Dual polarization cross slot with and without applied magnetic field. Data taken in a passive cooled dewar.

In all these experiments we have used a 100 MHz bandpass filter.

XI. Implications to Radio Astronomy

The results presented suggest that the mechanical perturbation of cryo-coolers can cause astronomical observations of narrow linewidth galactic sources to deviate from theory when integration's exceed $\sim$ 10 seconds (given a spectrometer frequency resolution of 1 MHz). Indeed, such behavior is often observed. In the past, the dominant source of such deviations has been believed to be variations in atmospheric opacity, referred to as sky-noise. Our results suggest that in some instances, especially under good sky conditions, the instrument itself may produce the limiting instabilities. The popular use of closed cycle LHe coolers is likely to aggravate the situation

with the introduction of small scale periodic temperature fluctuations in the mixer (Fig 7), this in addition to the acoustical noise effects discussed earlier.

On single aperture telescopes, the best way to avoid instability induced observing inefficiencies is to use a chopping secondary. This 'beam switching' technique allows the observer to switch between 'on' and 'off' source positions at frequencies up to several Hertz, thus largely eliminating the $1/f$ noise instabilities of the receiver system.

Note that such 'beam-switched' observations can only be used when the astronomical source emission region is no more than a few telescope beamwidths in extent. For more extended sources, an on-off position switching strategy is often employed. However, if the observers are limited to integration times of 10 seconds or less, they may find themselves spending more time slewing the telescope between positions than actually taking data. On the other hand, if integrations longer than 10 seconds are allowed, baseline subtraction suffers and integration efficiency is expected to be poor. An alternative observing mode is 'on-the-fly' (OTF) mapping. Here the telescope is allowed to scan through the source while averaging the data in short (typically ~ 3 sec) bins. When atmospheric conditions are good (≤ 1 mm of precipitable water vapor) 'on' scans can last for upwards of 120 seconds before a single 'off' scan is taken, thereby minimizing the loss in time associated with slewing the telescope between 'on' and 'off' positions. However, even when the 'OTF' mapping technique is used observing efficiency and proper baseline subtraction will improve if the receiver stability is increased.

When SIS receivers are used for large continuum or low resolution extragalactic observations only fast 'beam switching' operation seems appropriate.

Finally, it should be noted that interferometers (multiple telescope's used together to synthesize a single large diameter telescope) are by their nature much more tolerant of gain fluctuations than single dish receivers. This because only cor-

related signals will appear at the output of the spectrometer while uncorrelated signals such as receiver instabilities will not. Note however that this does not negate the importance of high integration efficiency, and hence having receivers with suitable long stability ("Allan" variance) times.

XII. Conclusion

A detailed study on the output noise stability of SIS receivers is presented. We have investigated the destabilizing effects of acoustic vibrations on a low noise amplifier (LNA) and local oscillator (LO) chain , micro-phonic noise on the LNA and SIS mixer bias lines, SIS constant voltage feedback bias noise, Josephson oscillation noise, and finally thermal drift noise of the SIS mixer and low noise amplifier.

In the process we found that fundamentally the SIS mixer is stable to at least 6 seconds in a 100 MHz bandwidth. This limit is set by how well one is able to suppress the Josephson effect in the superconducting tunnel junction and possibly also by SIS mixer bias noise, which modulates the mixer gain. In practice though the Josephson effect does not limit the stability of SIS receivers, rather the stability of the receiver is set by numerous external factors.

In a passive cooled dewar we have measured "Allan" variance stability times up to 9 seconds with an above the energy gap biased SIS mixer (IF bandwidth = 100 MHz). The "Allan" variance time in this case is limited by the room temperature IF total power amplifier and measurement setup.

In an active cooled hybrid style dewar the situation was much worse. With the low noise amplifier mounted on the 15K active cooled stage we measure an "Allan" variance time of 1.5 seconds, both at the observatory and in the laboratory. Vibration isolating the low noise amplifier gives a significant stability improvement, however the exact amount of improvement is very much dependent on the amplifier design and employed mounting scheme.

In the lab we did not observe a difference in the "Allan"

variance stability time of the receiver when the junction was biased in closed feedback, or open loop mode. At the observatory, due to the large EMI/RFI noise environment, we did in fact notice a significant change.

The mixer gain of a Local Oscillator pumped SIS junction has been measured and is observed to be a strong and negative function of temperature. The mixer's peak sensitivity to temperature change appears to be at approximately 4.9 Kelvin. The low noise amplifier (GaAs HEMT's) in contrast has a small, linearly varying, and positive temperature dependence. Cooling the mixer below 3K improves the mixer gain by 10%, but even more importantly reduces the mixer's susceptibility to LHe bath temperature fluctuations. In high resolution spectrometer mode with a channel bandwidth of 100 KHz, 1 second of "Allan" stability time and an high altitude Helium bath temperature of 3.6 Kelvin, we find a maximum allowed temperature fluctuation of 106 mK/second for the LNA and 48 mK/second for the SIS mixer. At 4.2 Kelvin the allowed SIS mixer temperature fluctuation has been reduced to 13.8 mK/second. These numbers are upper limits, and for wide bandwidth continuum or course resolution extragalactic observations the result is much more stringent.

Finally, high mobility transistor (HEMT) gain fluctuations, if any, appear to be at least an order of magnitude below such noise sources as acoustic vibrations, bias line noise due to high EMI/RFI noise environment, and problems with Josephson noise suppression.

It is recommended that special attention be given to minimize microphonic pickup in the LNA and Local Oscillator chain. Temperature fluctuations should be kept at a minimum, especially so when the mixer is operated at a Helium bath temperature of 4.2 Kelvin. In a high noise environment such as an observatory, it may be advisable to use several different feedback loop time constants, depending on the mode of operation. And finally a resistive divider network in the SIS and LNA bias line should at all cost be implemented.

XIII. Acknowlegments

We wish to thank Jonas Zmuidzinas and Frank Rice of Caltech for very helpful discussions on the fundamental physics of SIS mixers, Chris Walker of the University of Arizona, Dave Woody of Caltech, and John Carlstrom of the University of Chicago for their input regarding the implications of receiver instability to Radio Astronomy, and Sander Weinreb of JPL for his thoughts on LNA gain stability. This work was supported in part by NSF grant# AST-9615025.

References

[1] J.D. Kraus, "Radio Astronomy", *2nd Edition, pp7-8*

[2] D. W. Allan, "Statistics of Atomic Frequency Standards", *Proc. IEEE,* Vol. 54, No. 2, pp 221-230, 1969

[3] A.B Barnes, "Characterization of frequency stability", *IEEE Trans. Instrument Measurements,* Vol. IM-20, No. 2, pp 105-120, 1971

[4] R. Schieder, "Characterization and Measurement of System Stability", *SPIE, Vol 598,* Instrumentation for Submillimeter Spectroscopy (1985)

[5] B.D. Josephson, "Possible new effects in superconductive tunneling", *Phys. Letters 1,* (1962) pp 251-253

[6] R. Bradley, *NRAO,* Private Communication

[7] S. Padin, "A Cooled 1-2 GHz balanced HEMT amplifier", *IEEE, Microwave Theory and Techniques,* Vol 39, No. 7, pp. 1239-1243 (1991)

[8] *Infrared Laboratories, Inc.* 1808 East 17th Street, Tuscon, Az 85719

[9] B.N Ellison, "A low noise 230 GHz SIS receiver", *Int. J. Infrared and Millimeter waves,* Vol. 8, pp. 609-625, June 1987

[10] CTI-Cryogenics, Helix Technology Corporation, Nine Hampshire Street, Mansfield, MA 02048, USA.

[11] Personal communication

[12] G. Chattopadhyay, D. Miller, H. G. LeDuc, and J. Zmuidzinas, "A 550-GHz Dual Polarized Quasi-Optical SIS Mixer," *Proceedings of the Tenth International Symposium of Space Terahertz Technology*, Charlottesville, Virginia, pp. 130-143, March 16-18, 1999.

[13] J. W. Kooi , M. Chan, B. Bumble, and T. G. Phillips, "A low noise 345 GHz waveguide receiver employing a tuned 0.50 μm^2 Nb/AlO_x/Nb tunnel junction," *Int. J. IR and MM Waves,* vol. 15, No. 5, May 1994.

[14] J.W. Kooi, J. Pety, B. Bumble, C.K. Walker, H.G. LeDuc P.L. Schaffer, and T.G. Phillips, "A 850 GHz Waveguide Receiver employing a Niobium SIS Junction Fabricated on a 1um Si3N4 Membrane," *IEEE Transactions on Microwave Theory and Techniques,* Vol. 46, No. 2, pp151-161, February 1998.

SAC – Al Wooten

Al Wooten

Next: System Up: Report of the ALMA Previous: ALMA Liaison Group Issues

Receivers

Along with the telescopes, the receiver packages largely determine the capabilities of ALMA. The Joint Receiver Development Group (JRDG) has raised a number of questions and requested clarification from the ASAC. These may be broken down into questions concerning the frequency bands and their priority, the total power stability, the Water Vapor Radiometer (WVR) specifications (dealt with in a separate section), polarization requirements, calibration accuracy, and receiver configurations (principally single sideband versus double sideband operation). Recommendations for each of these areas are outlined below.
Frequency Bands. The ASAC concurs that the four bands to be initially installed on the array should be (in order of increasing frequency) Band 3 (86-116 GHz), Band 6 (211-275 GHz), Band 7 (275-370 GHz), and Band 9 (602-720 GHz). The ASAC reiterates that the frequency coverage should be as complete as possible, but we respond to the request for prioritization of the bands as follows.

- First Priority: Bands 3, 6, 7, and 9
- Second Priority: Bands 1, 4, and 2 (see below)
- Third Priority: Bands 5, 8, and 10

We strongly urge that the JRDG study the possibility of extending the lower frequency range of Band 3 to include the SiO maser transition near 86 GHz. If this is possible, Band 2 would drop to third priority. The frequency intervals of the other bands are reasonable. Band 10 is scientifically quite interesting. It is in the third priority because the technology of THz SIS heterodyne receivers is in an early state, and it will be difficult to make ALMA work at its highest operating frequency. Some delay in the installation of this band will enable the most sensitive receivers to be installed and the telescope performance to be optimized. Note that Band 1 is in the second priority list, and it must be considered in receiver layout. If it will not be in the main Dewar, then designs for optics that allow a second Dewar, possibly also containing the WVR, should be developed. It is not necessary for the WVR and Band 1 receivers to operate simultaneously.
Total Power Stability. For On-The-Fly (OTF) mapping capabilities, the requisite total power stability is of order 10^{-4} in one second (see Section 6, Appendix D). Stabilizing the gain to this level can be accomplished by selecting components with low temperature coefficients and by regulating their temperature to $\Delta T \leq 10^{-2}$ K. Regulating the rest of the electronics in the laboratory to that level will be difficult, and it might be best to use a (temperature regulated) total power detector on the front end for the continuum total power measurements, rather than trying to use the correlator as the continuum detector. The ASAC recommends that this level of gain stability be a goal, rather than a hard specification, pending further study. The over-riding concern is the receiver sensitivity, and better performance should not be sacrificed for stability at this stringent level. However, this level of stability may allow considerable simplication (avoiding nutating subreflectors, see section 6), and we encourage the JRDG to study the issue and report back to the ASAC on the prospects for achieving this level of stability and on possible tradeoffs in doing so. **WVR Specs**. These are discussed at length elsewhere (Section 7). The main point here is that this system must be incorporated into the overall design and receiver specifications.
Polarization. Polarization work will be an important part of ALMA research (Appendix C). Strong efforts should be made to have the polarized single-dish beams as stable as possible; consequently, the ASAC recommends that careful consideration be given to placing the 345 GHz receiver on-axis. For linear polarization work the basis state of feeds would ideally be circular polarization. If circular feeds impose important limitations on tuning range or increase significantly the noise temperature, a system for rapid,

Al Wooten

Next: System Up: Report of the ALMA Previous: ALMA Liaison Group Issues

Receivers

Along with the telescopes, the receiver packages largely determine the capabilities of ALMA. The Joint Receiver Development Group (JRDG) has raised a number of questions and requested clarification from the ASAC. These may be broken down into questions concerning the frequency bands and their priority, the total power stability, the Water Vapor Radiometer (WVR) specifications (dealt with in a separate section), polarization requirements, calibration accuracy, and receiver configurations (principally single sideband versus double sideband operation). Recommendations for each of these areas are outlined below.
Frequency Bands. The ASAC concurs that the four bands to be initially installed on the array should be (in order of increasing frequency) Band 3 (86-116 GHz), Band 6 (211-275 GHz), Band 7 (275-370 GHz), and Band 9 (602-720 GHz). The ASAC reiterates that the frequency coverage should be as complete as possible, but we respond to the request for prioritization of the bands as follows.

- First Priority: Bands 3, 6, 7, and 9
- Second Priority: Bands 1, 4, and 2 (see below)
- Third Priority: Bands 5, 8, and 10

We strongly urge that the JRDG study the possibility of extending the lower frequency range of Band 3 to include the SiO maser transition near 86 GHz. If this is possible, Band 2 would drop to third priority. The frequency intervals of the other bands are reasonable. Band 10 is scientifically quite interesting. It is in the third priority because the technology of THz SIS heterodyne receivers is in an early state, and it will be difficult to make ALMA work at its highest operating frequency. Some delay in the installation of this band will enable the most sensitive receivers to be installed and the telescope performance to be optimized. Note that Band 1 is in the second priority list, and it must be considered in receiver layout. If it will not be in the main Dewar, then designs for optics that allow a second Dewar, possibly also containing the WVR, should be developed. It is not necessary for the WVR and Band 1 receivers to operate simultaneously.
Total Power Stability. For On-The-Fly (OTF) mapping capabilities, the requisite total power stability is of order 10^{-4} in one second (see Section 6, Appendix D). Stabilizing the gain to this level can be accomplished by selecting components with low temperature coefficients and by regulating their temperature to $\Delta T \leq 10^{-2}$ K. Regulating the rest of the electronics in the laboratory to that level will be difficult, and it might be best to use a (temperature regulated) total power detector on the front end for the continuum total power measurements, rather than trying to use the correlator as the continuum detector. The ASAC recommends that this level of gain stability be a goal, rather than a hard specification, pending further study. The over-riding concern is the receiver sensitivity, and better performance should not be sacrificed for stability at this stringent level. However, this level of stability may allow considerable simplication (avoiding nutating subreflectors, see section 6), and we encourage the JRDG to study the issue and report back to the ASAC on the prospects for achieving this level of stability and on possible tradeoffs in doing so. **WVR Specs**. These are discussed at length elsewhere (Section 7). The main point here is that this system must be incorporated into the overall design and receiver specifications.
Polarization. Polarization work will be an important part of ALMA research (Appendix C). Strong efforts should be made to have the polarized single-dish beams as stable as possible; consequently, the ASAC recommends that careful consideration be given to placing the 345 GHz receiver on-axis. For linear polarization work the basis state of feeds would ideally be circular polarization. If circular feeds impose important limitations on tuning range or increase significantly the noise temperature, a system for rapid,

Next: Water-Vapor Radiometry **Up:** Report of the ALMA **Previous:** Configurations

Antennas and Total Power

The prototype antenna contractors have been selected. We therefore concentrated on recommendations for testing procedures and antenna issues that impact other areas. We considered the priorities when testing the prototype antennas. For the prototype tests, we stress the following points.

- It is extremely important to test whether and under what conditions the pointing specifications (06) are met. Developing observational strategies aimed at optimizing the pointing is an important goal. In particular, one should examine the possibility of installing optical telescopes on all antennas, together with a servo system allowing real time pointing corrections. It seems likely that such systems are only effective if they are planned as part of the system and the committee recommends therefore that a system of this type is considered soon.
- It is also very important to have some method of recovering zero spacing flux using all or part of the array operated in single dish mode (see Appendix D). The committee recommends that a detailed comparison be made of the relative merits of using nutators switching rapidly (10 Hz) and On-The-Fly (OTF) mapping. A decision on the best strategy for ALMA should be made subsequent to these tests. In particular, one should test whether rapid OTF mapping (e.g 30 scans in 1 sec with 1 second turn-around) is feasible and whether gain stability ($\Delta G/G$) of order 10^{-4} per second can be attained. Tests should also be made with the water vapor radiometer (WVR) in order to assess the ability of the WVR to monitor atmospheric emission fluctuations. Analogous studies are needed to test how effectively chopping with a simple nutator eliminates atmospheric fluctuations. Equipping each prototype antenna with a nutator will facilitate these studies. With this information in hand, it should be possible to decide whether nutators are, or are not, necessary for the array antennas. The general opinion of the ASAC was that if one could reach the scientific goals without using nutators, this was preferable. Thus one should aim at a system that could do an OTF map with all 64 antennas simultaneously.
- Polarization measurements are also sensitive to missing zero spacing flux (see Appendix C), and thus it should be possible to do polarization OTF at at least 2 ALMA frequencies. The decision discussed above (OTF versus nutators) may be different if one is measuring polarized flux and thus a test of polarization OTF is desirable.

Next: Water-Vapor Radiometry **Up:** Report of the ALMA **Previous:** Configurations

Al Wootten
2000-04-04

Next: Candidate Schemes **Up:** Total Power Observing with **Previous:** Total Power Observing with

Introduction

Particularly at the shorter wavelengths, the ALMA will need to do mosaic observing to cover large fields of view. Along with the mosaic pointing, there will need to be total power maps to fill in the interferometric short spacings and produce complete images. It is well known that this is best done with a single antenna that is two to three times the diameter of the interferometer antennas (Vogel,S. *et al* , ApJ, 1984, 283, 655). However, that will not be possible for ALMA; there are no 24m - 36m antennas available that will work well to 0.35mm wavelength. As long as a mosaic of pointings is employed in the interferometry, a single antenna map made with one of the interferometer antennas will suffice in principle (Ekers,R. and Rots,A, 1979, In Image Formation, etc., Dordrecht, Reidel). This is rarely done, largely because the interferometer antennas are not equipped to do it. Tests done at the VLA at cm wavelengths (Cornwell, T. 1988, A&A, 202, 316.) indicate that it should work, and at mm wavelengths in the CO(1-0) line, Marc Pound made a good map of the Eagle Nebula combining a Mosaic interferometer map made with the BIMA array and a single antenna map made with the Bell Labs 7m antenna (Pound, 1998, ApJ, 493L, 113). This capability must be in place for the ALMA antennas. How it is best done may be studied with the prototype antennas.

Next: Candidate Schemes **Up:** Total Power Observing with **Previous:** Total Power Observing with

Al Wootten
2000-04-04

next up previous

Next: OTF Mapping **Up:** Total Power Observing with **Previous:** Introduction

Candidate Schemes

There are five schemes that are usually considered for this purpose. The simplest is the on/off pointing method. Here one points at the source for a short integration, perhaps 10-30 seconds, and then at blank sky for the same time, and then takes the difference. The rest of the map results from a sequence of such measurements. For spectral line observations with narrow band widths, the receiver noise is usually large enough that it dominates both the atmospheric brightness fluctuations and the noise due to receiver gain fluctuations in this method, and it works. The second scheme is to use rapid frequency switching for spectral line observing, and this also works. Neither of these procedures will work for continuum measurements. That's obvious for the second method. For the first, the wider bandwidth means that the receiver noise is lower than that due to either the atmospheric brightness fluctuations or the effects of receiver gain fluctuations. For continuum total power observations, there are three schemes that can be used. The most common method is to employ a nodding secondary mirror. A related alternative is the focal plane chopper. The third idea is On-The-Fly mapping (Emerson, Klein, and Haslam, 1979, A&A, 76, 92). In all three cases, differential ground spillover will be a problem and will probably set the fundamental limit to the accuracy and depth of the continuum single antenna maps. The nodding secondary, giving a rapid comparison, avoids gain drifts. Its main weakness is that it is difficult to get a throw of more than a few arc minutes. While this will be adequate for some science programs, there are situations where one needs to chop to an ''off" position that is 10-20 (or more) minutes away. This is especially the case at the shorter wavelengths where, in the Milky Way, the background dust emission is bright. The focal plane chopper, on the other hand, can only throw large angles, typically 10 minutes or more. Other disadvantages for our application are that it is often difficult to have a good balance between the ''on" and ''off" and the mechanism would probably have to be mounted on each receiver separately, which could be an annoying complication for the ALMA antennas with their many receivers. The On-The-Fly (OTF) method looks to be the most flexible and simplest, and we summarize its properties and requirements below. Whatever scheme is chosen, the maximum throw will limit the maximum spatial scales in the resulting maps.

next up previous

Next: OTF Mapping **Up:** Total Power Observing with **Previous:** Introduction

Al Wootten
2000-04-04

next up previous

Next: Summary **Up:** Total Power Observing with **Previous:** Candidate Schemes

OTF Mapping

The prospects for doing OTF mapping at the Chajnantor site have been discussed in detail by Holdaway, Owen, and Emerson (1995, MMA #137) (HOE). The basic idea is that a raster scan of the object under study will be made with a very rapid turn-around of the scan at the end of each row in a region that is off the source. During the scan across the source, the receiver power is read out at a rate which corresponds to at least the Nyquist sampling of the source structure. That is, at least as often as twice per beam width. Thus, there are many ''on" observations across the source with an ''off" observation at the end of each row. The ''off" observations last about one second during the turn-around at the end of each row. The time on each ''on" observation is much smaller. HOE used the path length fluctuations as measured by the site testing interferometer at Chajnantor to infer the expected atmospheric brightness fluctuations. They were able to work out the magnitude of the fluctuations as functions of both the time and pointing angle with respect to the source. Under the assumptions that (1) the antenna could slew as rapidly as 1^o/second, (2) the antenna could accelerate and decelerate between normal tracking and full slew in one or two seconds, and (3) the correlator could dump the spectral data every .003s, they concluded that OTF mapping should work well at the Chajnantor site. Their Figure 2 shows that the expected receiver noise and atmospheric noise contributions will be about equal at 230 GHz 80% of the time for a scan that is a large as 1^o. For smaller scans the situation is even better. At the time of the HOE memo, is was not clear whether their assumptions about the antenna and correlator would be met. We now have more information about the array components. The present NRAO design for the correlator will allow correlator read-out at the rate of once every .001 second, which is fast enough to permit OTF mapping of both continuum and line observations (J. Weber, private communication). The planning for the antenna prototype has included studies of the capability of the antenna to carry out the OTF observing. It appears that if feed forward is used in the drive servo design, it will be possible to turn the antenna around at the end of an OTF scan in about one second as assumed by HOE. The maximum smooth scan rate will be at least about 0.5^o/sec, comparable to the 1^o/sec rate assumed by HOE. One further point that needs to be considered is the required receiver gain stability for the OTF scheme to work. The planned continuum bandwidth of 8 GHz calls for unusually good gain stability. The time between any of the ''ons" and the off at the end of the scan is about one second. The gain must be stable over that time interval. The fractional total power noise for one of the ''on" measurements is: $\Delta T/T = 2/SQRT(Bt_s)$. B is the bandwidth, and t_s is the time on each source. The 2 is the usual factor due to switching. Here the long ''off" time reduces the noise in the subtraction, but it is also about twice as long as the total ''on" source observing time. The fractional total power fluctuation due to gain variations is: $\Delta T/T = \Delta G/G$. If we take the scan time to be always one second, then t_s depends on the scan length and the beam width. For scan lengths between 5' and 60' and beam widths between 25'' (220 GHz) and 6'' (800 GHz) the time on source varies between .08 sec and .002 sec. For B=8 GHz, and equating the receiver noise fluctuation to that due to the gain fluctuation, we find a necessary gain stability in the range of 0.8×10^{-4} to 5×10^{-4}. Thus, a receiver gain stability of about 1×10^{-4} over a time scale of about 1 second is required for the receiver. This level of stability can certainly be achieved, but it requires careful attention to the construction of the receiver. The above argument leading to a gain stability requirement of 1×10^{-4} depends on the relative time on each ''on'' during the scan being small compared with the total scan time of about 1 second. Thus, the OTF method works best for large scans (M. Wright, private communication). Even for short scans, it will still work reasonably well, requiring a little more gain stability. It will be important to keep the total scan time to be about the same

time as the turnaround time, in order that the overall observing be efficient. Another question concerns the number of antennas that must be used to achieve the necessary sensitivity in the single antenna measurements to equal the corresponding array sensitivity. The answer here depends on the amount of redundancy in the short interferometer spacings. If there is no redundancy in the short interferometer spacings, then, for approximately equal sensitivity in the OTF measurements, the same amount of time must be spent on the single dish map as on any of the array baselines. That means about the same amount of time in the single dish mode as in the array mode. The only difference is in the factor of 2 in the OTF (switched) mode. This implies that a measurement with 4 antennas for the same duration as the array observation would suffice. However, with the likely large redundancy in the short interferometer spacings, much more time in the single dish mode will be required. Exactly how much time will depend on the details of the compact interferometer array. Probably most of the antennas will be required to operate in the single antenna mode simultaneously to produce the uv plane sensitivity comparable to the of the array. The requirement that all the antennas have the good gain stability makes the most sense. It is not a difficult requirement, and it will benefit the interferometer operation as well.

Next: Summary **Up:** Total Power Observing with **Previous:** Candidate Schemes

Al Wootten
2000-04-04

Next: 183GHz Water Vapour Radiometers **Up:** Total Power Observing with **Previous:** OTF Mapping

Summary

The major limitation in the accuracy of the single dish mode will be due to differential spillover in the ''on''-''off'' comparison. It is difficult to know in advance whether the nodding secondary or the OTF scanning scheme will be more plagued by this. The antenna background is likely to be of the order of 10K. Whether the modulation of this by the moving secondary or scanning across the ground is worse can only be determined by experiment. Thus, it will be important that the prototype antennas be equipped for both kind of observing and tests be carried out. Both good gain stability and chopping secondaries must be installed. It may be possible to test these options on existing systems. It may also be possible to test further the ''homogeneous array'' operation (array with single dish one of the array antennas) using one of the existing antenna systems. Another activity that would be important in the near term would be to test the calculations of HOE with atmospheric data taken at higher frequencies. The atmospheric conditions on Mauna Kea are probably close enough to those at Chajnantor that JCMT observations would be useful for this. Among all the possible methods to obtain the total power data for the array, the OTF scheme is the simplest and least expensive, and it appears that it should work. The main requirement is a fractional receiver gain stability of about 1×10^{-4} in a one second time interval for all the antennas. There should be no difficulty in achieving this.

Next: 183GHz Water Vapour Radiometers **Up:** Total Power Observing with **Previous:** OTF Mapping

Al Wootten
2000-04-04